Institutionen för systemteknik
Department of Electrical Engineering

Examensarbete

Extended LTE Coverage For Indoor Machine Type Communication

Examensarbete utfört i Kommunikationssystem
vid Tekniska högskolan vid Linköpings universitet
av

Joel Berglund

LiTH-ISY-EX--13/4683--SE

Linköping 2013

Linköpings universitet
TEKNISKA HÖGSKOLAN

Department of Electrical Engineering
Linköpings universitet
SE-581 83 Linköping, Sweden

Linköpings tekniska högskola
Linköpings universitet
581 83 Linköping

Extended LTE Coverage For Indoor Machine Type Communication

Examensarbete utfört i Kommunikationssystem
vid Tekniska högskolan vid Linköpings universitet
av

Joel Berglund

LiTH-ISY-EX--13/4683--SE

Handledare: **Pål Frenger**
Ericsson Research
Erik Eriksson
Ericsson Research
Anton Blad
ISY, Linköpings Universitet

Examinator: **Danyo Danev**
ISY, Linköpings Universitet

Linköping, 20 juni 2013

Titel
Title

Utökad LTE-Täckning För Maskintypskommunikation Inomhus

Extended LTE Coverage For Indoor Machine Type Communication

Författare
Author

Joel Berglund

Sammanfattning
Abstract

The interest of *Machine Type Communication* (MTC) is increasing and is expected to play an important role in the future network society. In the process of increasing the number of connected devices, the coverage plays an important role. This thesis work aims to study the possibility of supporting coverage limited MTC-devices within LTE by extending the LTE coverage.

It shows that coverage increase by means of repetition is a good candidate, which allows for a significant increase without hardware upgrades at a low cost in terms of radio resources. For inter-site distances up to 2500 m, the proposed repetition scheme with an increase of 20 dB allows for almost complete coverage where today's LTE have significant lack of coverage. It also shows that even though the increased coverage implies higher resource usage, the limitation is not in the number of users supported, but rather the coverage at longer inter-site distances.

Nyckelord
Keywords   LTE, 4G, MTC

Abstract

The interest of *Machine Type Communication* (MTC) is increasing and is expected to play an important role in the future network society. In the process of increasing the number of connected devices, the coverage plays an important role. This thesis work aims to study the possibility of supporting coverage limited MTC-devices within LTE by extending the LTE coverage.

It shows that coverage increase by means of repetition is a good candidate, which allows for a significant increase without hardware upgrades at a low cost in terms of radio resources. For inter-site distances up to 2500 m, the proposed repetition scheme with an increase of 20 dB allows for almost complete coverage where today's LTE have significant lack of coverage. It also shows that even though the increased coverage implies higher resource usage, the limitation is not in the number of users supported, but rather the coverage at longer inter-site distances.

Acknowledgments

This thesis work has been done at Ericsson Research in Linköping, Sweden, during the spring semester 2013.

Contents

Symbols & Abbreviations

SYMBOLS

Symbol	Meaning
$a_k^{(m)}$	Symbol of the kth carrier and mth symbol interval
A_k	Amplitude of symbok k
B	Bandwidth
C	Capacity
dl_{oh}	The amount of overhead in an downlink RB pair
β_{PRACH}	Amplitude scaling for PRACH
Δf	Frequency spacing
Δf_{RA}	Subcarrier spacing for the random access preamble
f_{c}	Carrier frequency
$d_{k,}^{(i)}$	The ith output stream from the turbo coder of block k
$v_k^{(i)}$	The ith output stream after the interleaver of block k
w_k	The sequence of bits in the circular buffer
e_k	The sequence of bits after selection and pruning
ϕ	Phase difference
τ	Time delay
θ	Total phase difference
σ	Noise variance
F_{dl}	Noise figure in downlink
F_{ul}	Noise figure in uplink

Symbol	Meaning
G	Geometry in downlink
g_i	The ith pathgain
L	Path loss
N_{ZC}	Length of Zadoff-Chu sequence
N_c	Number of coherent accumulations
N_{dl}	Noise power in downlink
N_{nc}	Number of non-coherent accumulations
N_{ul}	Noise power in uplink
P_{eNB}	Maximum output power by an eNodeB
$p_{\text{miss/falsedetection}}^{\max}$	Desired maximum probability for a miss/false detection of a preamble
R_{average}	Average number of preambles used
R_k	Average number of preambles used by user k
T_{CP}	Duration of the cyclic prefix
T_d	Coherence time
T_s	Basic time unit
T_{SEQ}	Duration of the Zadoff-Chu sequence for preamble
T_u	Symbol time
ul_{oh}	The amount of overhead in an uplink RB pair
x_u	The uth root Zadoff-Chu sequence

Abbreviations

Abbreviation	Meaning
3GPP	Third Generation Partnership Project
ACK	Acknowledgement (in ARQ protocols)
ARQ	Automatic Repeat-reQuest
AWGN	Additive White Gaussian Noise
BCH	Broadcast Channel
BLER	Block-Error Rate
BSC	Base Station Controller
BTS	Base Transceiver Station
C-RNTI	Cell RNTI
CDF	Cumulative Distribution Function
CN	Core Network
CoMP	Coordinated Multi-Point transmission and reception
CRC	Cyclic Redundancy Check
CRS	Cell-Specific Reference Signals
DFT	Discrete Fourier Transform
DFTS-OFDM	DFT-Spread OFDM
DL-SCH	Downlink Shared Channel
DM-RS	Demodulation Reference Signals
eNodeB	E-UTRAN NodeB
EPA	Extended Pedestrian A
EPC	Evolved Packet Core
EPS	Evolved Packet System
E-UTRAN	Evolved UTRAN
FDD	Frequency Division Duplex
FFT	Fast Fourier Transform
FIR	Finite Impulse Response
GPRS	General Packet Radio Service
GSM	Global System for Mobile communications
HARQ	Hybrid ARQ
HSPA	High Speed Packet Access
IIR	Infinite Impulse Response
IMT-Advanced	International Mobile Telecommunications Advanced (ITU's name for the family of 4G standards)
IP	Internet Protocol
ISD	Inter-Site Distance
ITU	International Telecommunications Union
LTE	Long-Term Evolution
MAC	Medium-Access Control
MBSFN	Multicast-Broadcast Single-Frequency Network
MCS	Modulation and Coding Scheme
MIB	Master-Information Block
MIMO	Multiple-Input Multiple-Output
MME	Mobility Management Entity

ABBREVIATIONS

Abbreviation	Meaning
MTC	Machine Type Communication
NAS	Non-Access Stratum
NodeB	A logical node handling transmission/reception in multiple cells
OFDM	Orthogonal Frequency-Division Multiplexing
PBCH	Physical Broadcast Channel
PDCCH	Physical Downlink Control Channel
PDCP	Packet Data Convergence Protocol
PDSCH	Physical Downlink Shared Channel
PHICH	Physical Hybrid-ARQ Indicator Channel
PHY	Physical Layer
PRACH	Physical Random-Access Channel
PSS	Primary Synchronization Signal
PUCCH	Physical Uplink Control Channel
PUSCH	Physical Uplink Shared Channel
QAM	Quadrature Amplitude Modulation
QPP	Quadrature Permutation Polynomial
QPSK	Quadrature Phase-Shift Keying
RA	Random Access
RACH	Random-Access Channel
RAN	Radio-Access Network
RB	Resource Block
RLC	Radio-Link Control
RNC	Radio Network Controller
RNTI	Radio-Network Temporary Identifier
RRC	Radio Resource Control
RTT	Round-Trip Time
SFN	System Frame Number
S-GW	Serving Gateway
SIB	System-Information Block
SINR	Signal-to-Interference-and-Noise Ratio
SI-RNTI	System Information RNTI
SNR	Signal-to-Noise Ratio
SRS	Sounding Reference Signals
SSS	Secondary Synchronization Signal
TDD	Time-Division Duplex
TC-RNTI	Temporary Cell RNTI
TM	Transmission Mode
TTI	Transmission Time Interval
UE	User Equipment (the 3GPP name for the mobile terminal)
UL-SCH	Uplink Shared Channel
UMTS	Universal Mobile Telecommunications System
UTRAN	Universal Terrestrial Radio Access Network

1

Introduction

Wireless communications have become indispensable to modern life. The possibilities of constant internet access have had a tremendous impact on our daily lives. It is getting cheaper and more convenient with connectivity which creates great opportunities for different markets for increased effectiveness and reduced costs.

As an example of non-human centric applications, cheap connected devices can, for everything from power companies to health care, enable remote monitoring, allowing improved utilization of human resources which leads to reduced costs and increased quality.

Ericsson has set out a vision of more than 50 billion connected devices by 2020 [15], where 3 billion of them will be different types of utility meters. These devices are classified as *Machine Type Communication* (MTC) devices and are increasing in popularity. MTC-devices differ quite much from human centric devices in terms of requirements. They typically have quite modest requirements in terms of data rate and delay which can be served well by GSM/GPRS, but as more MTC-devices are deployed, the reliance on GSM/GPRS increases, which increases maintenance costs of operating several *Radio Access Technologies* (RAT's).

With users and traffic becoming denser, using more spectral efficient technologies, such as *Long Term Evolution* (LTE), allow the operators to utilize their spectrum in a much more efficient way. Since MTC-devices typically lack mobility, some might end up at positions with permanent poor channel conditions. For such devices, e.g. utility meters in basements, a large increase in SNR may be needed for sufficient coverage. The high costs from solutions such as deploying additional base stations or relay nodes are difficult to justify since the aim is increased coverage for low-end devices which are supposed to operate at low cost.

This thesis aims to evaluate the possibility of expanding the coverage with 20 dB [21] and extract the coverage and the number of users supported. As the biggest challenge in the coverage enhancement is the uplink [12], the simulations are focused on the uplink signaling, such as the *Physical Random Access Channel* (PRACH) and the *Physical Uplink Shared Channel* (PUSCH).

1.1   Outline

In Chapter 2, some basic information about LTE is presented with deeper focus on certain more relevant aspects to this thesis.

Chapter 3 presents ideas of possible changes to todays LTE in order to allow for coverage enhancements.

In Chapter 4, the simulations performed in this thesis are presented along with the results. The results are also discussed and analyzed and put in relation to the ideas from chapter 3.

In Chapter 5, the conclusion of the results are discussed in relation to previous chapters, with a focus on the most important outcomes, what data rate can be achieved and how many coverage limited MTC-devices can be supported.

2

LTE Overview

This chapter introduces LTE with higher focus on the physical layer aspects. Readers who are already familiar with LTE may skip this chapter and proceed to chapter 3.

LTE is a 4G-standard for mobile communication developed by *3rd Generation Partnership Project* (3GPP) for packet-switched high-speed data transfer, and was designed to substitute 2G/3G standards such as GSM/UMTS. In 2004, the work on LTE began and first, requirements were set out with aims on peak rate and spectrum flexibility [1]. The requirements were followed by work on developing the different radio technologies which lead to the first release, release 8, in 2008, and the first commercial network operation started in 2009.

In late 2009, release 9 came out with additional features such as Multicast/Broadcast Support, support for network assisted positioning and improved beamforming in downlink. With release 10 in late 2010, LTE was referred to as LTE-Advanced after fulfilling ITUs requirements IMT-advanced [18]. On top of that, 3GPP set out their own requirements [7] which extended the requirements as well as adding new ones. One important requirement from [7] was backwards compatibility such that earlier release terminals could access carriers supporting LTE release-10. From then on, the work has continued on newer releases with further improvements with release 11 being the latest (June 20, 2013).

This thesis work covers ideas for a possible feature for LTE release 12. The information in this chapter comes from [14] if no other source is mentioned.

2.1 System Architecture Overview

The overall system architecture used in LTE is quite different compared to earlier standards such as GSM and UMTS/HSPA. In the development of LTE, the *Radio-Access Network* (RAN) and the *Core Network* (CN) were revisited and resulted in a flat RAN architecture and a new core network, *Evolved Packet Core* (EPC) which is packet-switched only, as compared to the GSM/GPRS core network. The RAN is responsible for all radio related functionalities while the EPC is responsible for non-radio related functionalities needed for a full mobile-broadband network. Such functionalities involves for example authentication and customer charging functionality. The LTE RAN and the EPC are together referred to as *Evolved Packet System* (EPS).[1]

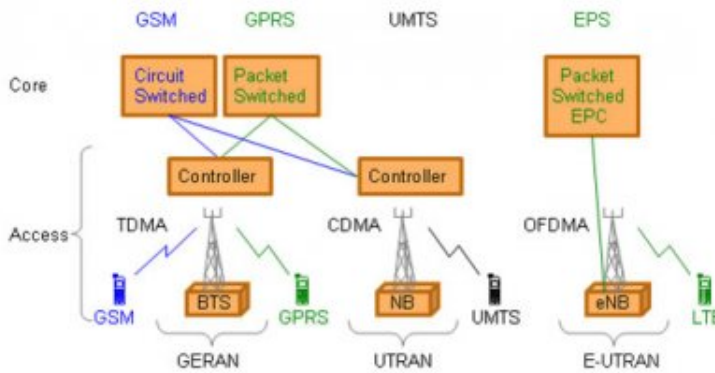Figure 2.1 illustrates some fundamental differences between the architectures in LTE and earlier standards.

Figure 2.1: *Structure in GSM, GPRS, UMTS and LTE.*

In GSM, there are two nodes between the terminals and the core network. The terminals are connected to *Base Transceiver Stations* (BTS) who are controlled by *Base Station Controllers* (BSC). Each BSC is connected to several BTS and the functionality of the BSC involves for example, allocation of radio channels and handover between BTS.

In UMTS, the setup of nodes between the terminals and the core network is similar to GSM. In UMTS, the terminals are connected to *NodeB*s which are controlled by *Radio Network Controllers* (RNC).

In the LTE RAN, the *Evolved Universal Terrestrial Radio Access Network NodeB* (eNodeB) is the only node between the terminal and the EPC. It handles all functionality corresponding to both the NodeB and the RNC. The functionality operating between the terminal and the EPC is referred to as the *Non-Access Stratum* (NAS). As can be seen in Figure 2.2, the connection between the eNodeB and the EPC

---

[1]UTRAN is also a part of the EPS

is done through the *S1 interface*. The user-plane part to the *Serving Gateway* (S-GW) is done with the S1-u interface and the control-plane part to the *Mobility Management Entity* (MME) is done with the S1-c interface. The eNodeBs can communicate with each other through the X2 interface.

The S-GW is the user-plane node connecting the EPC to the LTE RAN. It works as a mobility anchor when a terminal is moving between eNodeBs and collects statistics for the charging functionality.

The MME is the control-plane node connecting the EPC to the LTE RAN. Responsibilities of the MME involves for example connection/release of bearers to a terminal, transitions from IDLE to ACTIVE and security key handling.
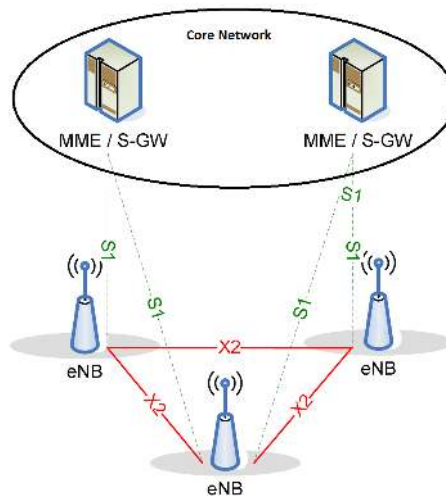

Figure 2.2: Illustration of the RAN-interfaces [6].

2.2   Protocol Architecture and Channels

This section gives a brief illustration of the RAN structure followed by a brief presentation of the channels on the mentioned layers.

In LTE, a number of radio bearers are defined to which the higher layer packets are mapped according to their Quality-of-Service requirements. A general overview of the user-plane protocol structure is illustrated in Figure 2.3 and the control-plane protocol structure in Figure 2.4 [6]. Note that the MME does not belong to the RAN.

Control messages for terminals can originate either from the MME or the *Radio Resource Control* (RRC). The RRC is located in the eNodeB and handles RAN-

related procedures such as broadcasting of system information, transmission of paging messages, connection management and mobility functions.
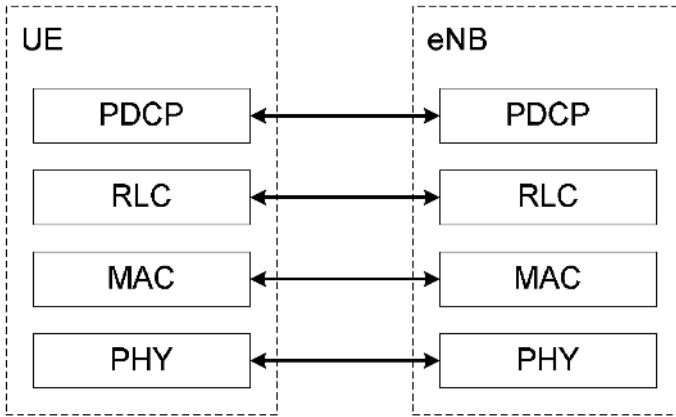

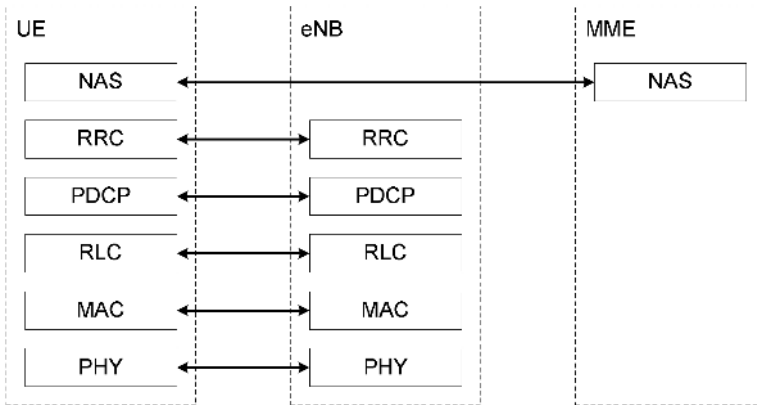*Figure 2.3: Illustration of the user-plane protocol stack [6].*

Figure 2.4: Illustration of the control-plane protocol stack [6].

Figure 2.3 illustrates the user-plane layers which are briefly described below:

- The *Packet Data Convergence Protocol* (PDCP) is among other things used for ciphering and header compression for the higher layer packets. The compression is done since the structure of the headers in the higher layers allows for a significant compression.

- The *Radio-Link Control* (RLC) is mainly responsible for segmentation/concatenation and retransmission handling. It offers services in the form of *radio bearers* to the PDCP.

- The *Medium-Access Control* (MAC) handles the multiplexing of logical channels, hybrid-ARQ retransmissions, and uplink and downlink scheduling.

The scheduling functionality is handled by the eNodeB for both uplink and downlink. The MAC-layer offers services to the RLC in the form of *logical channels*.

- The *Physical Layer* (PHY) handles lower layer functionality such as coding/decoding, modulation/demodulation and multi-antenna mapping. The physical layer offers services to the MAC-layer in the form of *transport channels*.

On the lowest level there are also a number of physical channels defined. The logical and transport channels defined in downlink and uplink are illustrated in Figure 2.5 [6].
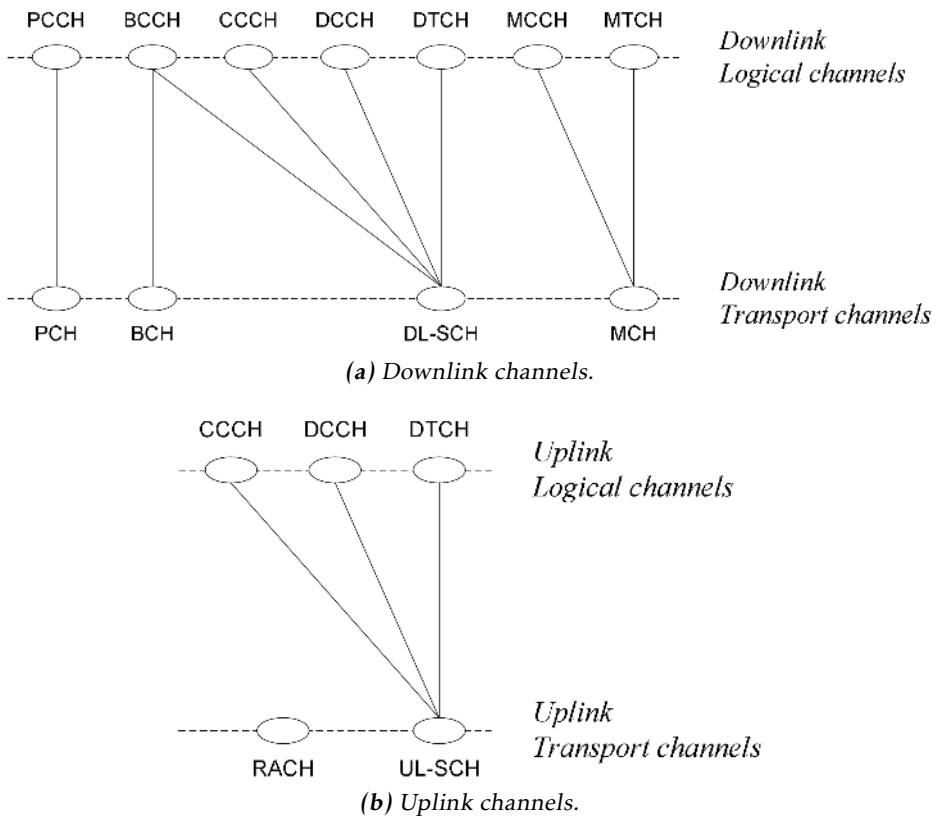

(a) Downlink channels.

(b) Uplink channels.

Figure 2.5: *Illustration of logical and transport channels in downlink and uplink.*

The transport channels of interest in this thesis in both downlink and uplink are:

- The *Broadcast Channel* (BCH) is used for broadcasting of some limited amount of system information.

- The *Downlink Shared Channel* (DL-SCH) is the main transport channel in

the downlink. It allows for key features in LTE such as dynamic rate adaptation, channel dependent scheduling, hybrid ARQ with soft combining and spatial multiplexing.

- The *Uplink Shared Channel* (UL-SCH) is the corresponding uplink version of the DL-SCH.

- The *Random-Access Channel* (RACH) is used for the random-access procedure which will be described in Section 2.4.2.

and the physical channels of interest in this thesis are:

- The *Physical Downlink Shared Channel* (PDSCH) is the main channel for unicast transmissions (data specified to a specific terminal).

- The *Physical Downlink Control Channel* (PDCCH) is used for different types of control information in the downlink such as scheduling decision and scheduling grants enabling transmission on the PUSCH.

- The *Physical Broadcast Channel* (PBCH) carries the information broadcasted in the BCH.

- The *Physical Uplink Shared Channel* (PUSCH) is the uplink version of the PDSCH.

- The *Physical Uplink Control Channel* (PUCCH) is used for hybrid-ARQ acknowledgments, sending channel state reports and requesting scheduling on the PUSCH.

- The *Physical Random-Access Channel* (PRACH) is used for the random-access procedure which will be described in Section 2.4.2.

2.3 Physical Layer

This section covers some physical layer aspects and some connections to higher layers.

In the downlink, LTE is based on conventional *Orthogonal Frequency-Division Multiplexing* (OFDM). OFDM is a multicarrier transmission scheme, where each adjacent pair of carriers are separated $\Delta f = 1/T_{\mathrm{u}}$, where T_{u} is the symbol time. The baseband notation for an OFDM-symbol during the time interval $mT_{\mathrm{u}} \leq t < (m+1)T_{\mathrm{u}}$ can be expressed as:

$$\sum_{k=0}^{L-1} x_k(t) = \sum_{k=0}^{L-1} a_k^{(m)} e^{j2\pi k \Delta f t} \tag{2.1}$$

where $a_k^{(m)}$ is the symbol for the kth carrier during the mth symbol interval and L is the number of subcarriers. By having the relation $\Delta f = 1/T_{\mathrm{u}}$ between carrier

spacing and symbol time, all subcarriers are orthogonal to one another. This can be verified by calculating the inner product between two subcarriers.

The different carriers are usually illustrated in a time-frequency grid as shown in Figure 2.6.
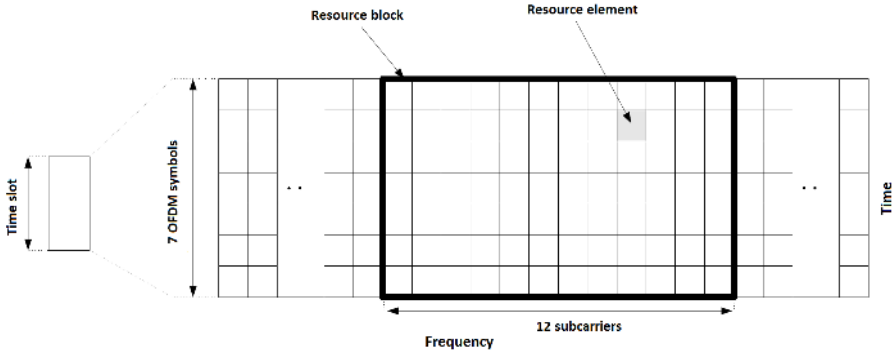

Figure 2.6: Time-frequency grid [3].

Also the uplink is based on OFDM. The OFDM-modulator is in the uplink preceded by a DFT-precoder. This is denoted *DFT-spread OFDM* (DFTS-OFDM). The reason for the pre-coder operation is to minimize the cubic metric to make the amplifier in the terminal more efficient.

In LTE, the carrier spacing is 15 kHz[2] which means that the symbol time is $T_u = 1/\Delta f = 1/(15 \cdot 10^3)$ s $= 66.7$ μs. Time entities are often expressed in the basic unit $T_s = 1/(15000 \cdot 2048)$ s. T_s can be seen as the sampling rate of an FFT-based transmitter/receiver in the case of an FFT size of 2048. An OFDM-symbol is thus $2048 T_s$. A slot is defined as 0.5 ms. As can be noticed, the time of a slot is not divisible by the time of an OFDM-symbol, which is explained by cyclic prefixes.

A cyclic prefix is an extension of a symbol and is used to retain orthogonality also for delayed versions of the received signal. The last samples of an OFDM-symbol corresponding to the time of the cyclic prefix, T_{CP} are copied to the beginning of the symbol so that the whole transmission of a symbol consists of a cyclic prefix and the symbol.

The smallest physical entity in LTE is called a *resource element* and is a subcarrier during one OFDM-symbol. It is thus 66.7 μs in time and 15 KHz in frequency. 12 resource elements in frequency during one time slot is called a *resource block* (RB). Two consecutive resource blocks in time is called a *resource-block pair*. Each slot can contain either 6 or 7 OFDM-symbols, depending on the length of the cyclic prefix.

The smallest entity in time to be scheduled is a subframe, which is two time slots. Ten subframes constitutes a radio frame, which therefore is 10 ms long.

---

[2]There is also a reduced subcarrier spacing, which is 7.5 KHz

The frames are identified on a higher layer by the *System Frame Number* (SFN) and has a period of 1024 frames, which is approximately 10 seconds. Each downlink subframe can be said to be divided into a *control region*, followed by a *data region*. The control region normally consists of 1–4 OFDM-symbols and carries associated downlink control signaling.

2.3.1   Reference Signals

In wireless transmissions, reference signals are often used, e.g. in order to estimate the channel for coherent decoding and making good scheduling decisions. Reference signals, or pilot symbols are predefined symbols, known to the receiver, which gives channel information at a given time instance for certain frequencies, which makes the decisions in the decoding more reliable. eNodeBs schedule users at appropriate frequencies with suitable modulation and coding schemes based on the channel-state reports from the terminals. In downlink, there are different kinds of reference signals for different purposes and two of them are described below.

Cell-Specific Reference Signals (CRS) are transmitted in every downlink subframe in every resource block. As the name suggests, it is cell specific and is intended for all terminals in the same cell in order to decode cell-specific information as well as for making channel quality estimates. In every cell, there are as many cell-specific reference signals as there are antenna ports. When transmitting from several antenna ports, all the reference signals for the corresponding antenna ports are contained in the resource blocks. Figure 2.7 illustrates the position of a cell specific reference signal in a resource-block pair.
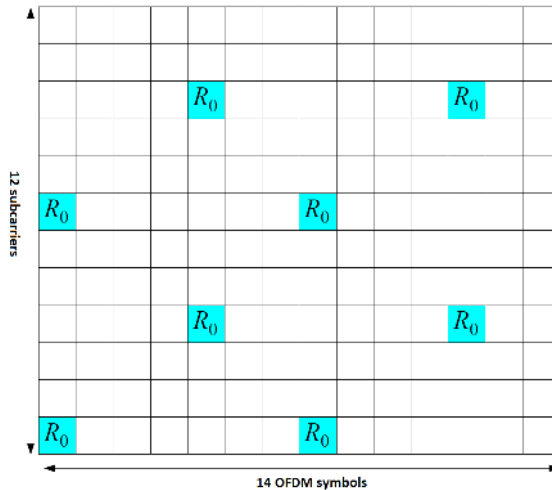

Figure 2.7: *Reference signal for one antenna port in a resource-block pair in downlink [3].*

Demodulation Reference Signals (DM-RS) are intended for specific terminals for

channel estimation on PDSCH transmissions in the case where CRS are not used.

In the uplink there are two kinds of reference signals, which are described below:

Uplink DM-RS are used by the base station for coherent demodulation of data from the PUSCH. A big difference between downlink and uplink DM-RS are the positioning of the symbols. In the case of downlink they are fairly spread among time and frequency, while in uplink, certain OFDM-symbols are used only for the DM-RS as shown in Figure 2.8. There are typically two OFDM-symbols for uplink DM-RS per RB pair.
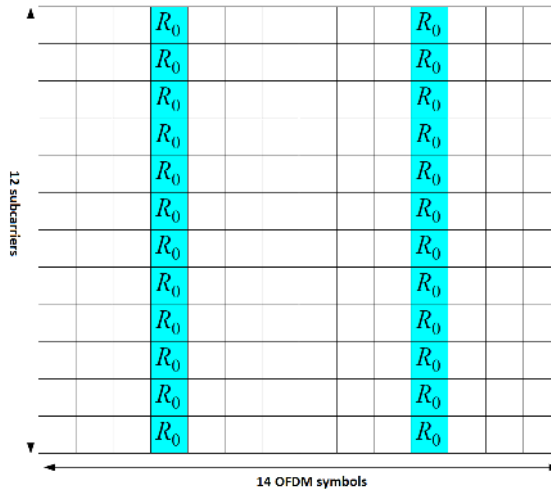

Figure 2.8: *Demodulation reference signal in uplink.*

Uplink *Sounding Reference Signals* (SRS) are used by the base station for estimation of the channel at different frequencies. These will be used by the base station when making decision on the scheduling for different users as well as for link adaptation.

As previously described, the base station will use the SRS and the channel-state reports from the terminals to make decisions on the link adaptation and scheduling. Since different users experience different channel variations, the terminals should be scheduled at frequencies with best momentary condition. Figure 2.9 illustrates how the channel condition for different users can vary.

The modulation order and coding rate is something that will affect the throughput and is therefore also decided based on the reference signals. For a certain condition, a particular choice of modulation and coding might perform better than other choices which means that it is important to adapt according to the current link conditions.
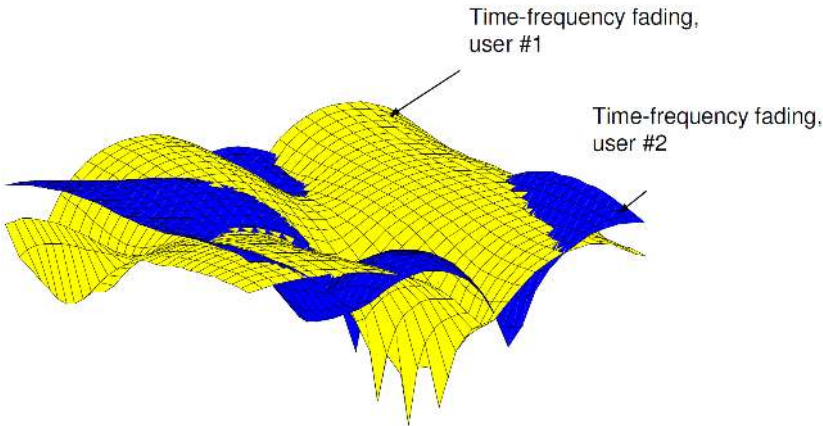
Figure 2.9: Example of fading for different users [17].

2.3.2   Transmission

This section will make a brief summary of some of the steps when transmitting data.

At first, a 24-bit *Cyclic Redundancy Check* (CRC) is appended to each transport block coming from the MAC-layer. The CRC is calculated from the transport block and allows for the receiver to detect if any error has occurred.

The next step is code block segmentation, which is done since the maximum size supported in the Turbo encoder is 6144 bits, due to the internal interleaver size. If the transport block including the CRC is larger than 6144 bits, it is segmented into smaller blocks where each block gets an additional CRC of length 24 bits appended. These code blocks are then handled by the Turbo encoder.

The Turbo encoder consists of two rate-1/2 eight-state constituent encoders, where the systematic bits are only used from the first encoder, implying an overall rate of 1/3. Between the two encoders is a *Quadrature Permutation Polynomial* (QPP) interleaver which interleaves the bits.

The next step is rate matching and the physical layer HARQ functionality. The output bits from the Turbo encoder are first separately interleaved and then inserted in a circular buffer with the systematic bits first, and then the parity bits alternating. The rate matching is then done by extracting the number of bits which are to be sent within a given subframe. Figure 2.10 illustrates how it is performed.

$d_k^{(i)}$ is the ith output stream from the turbo coder and $v_k^{(i)}$ is the result after interleaving. w_k is the sequence of bits in the circular buffer and e_k is the sequence of bits after selection.

After the rate matching, the bits are multiplied (exclusive-or) by a *scrambling*
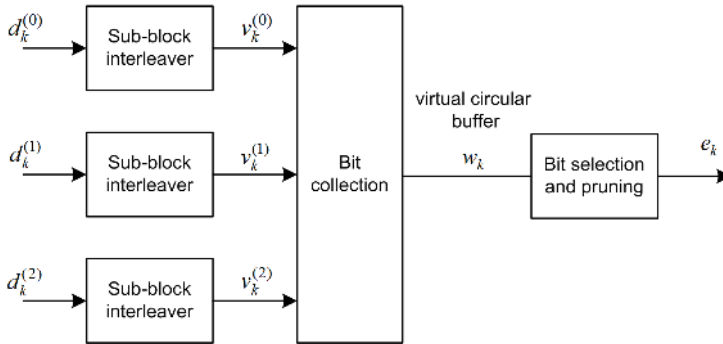
Figure 2.10: *Illustration of the steps from interleaving to rate matching [4].*

sequence. This allows for interfering signals to behave more like randomized noise which helps suppressing the impact of inference.

The next step involves transforming the scrambled bits into modulation symbols, which in LTE are QPSK, 16QAM and 64QAM corresponding to 2, 4 and 6 bits per symbol.

The last step involves antenna mapping and resource-block mapping where the symbols are mapped to certain antenna ports and then to specific resource elements within the resource blocks. Since a few of the resource elements will be occupied for different types of signalling in the downlink, not all 84 resource elements in a block are available for the downlink transport channels. The same applies for both uplink and downlink when it comes to reference signals.

As already described, the redundancy versions for HARQ is generated in the physical layer, but the HARQ protocol is on the MAC-level. It uses several parallel stop-and-wait processes.

2.4   Connection Establishment

This section covers the steps from terminal startup to an established connection.

2.4.1   Cell Search

When a terminal is first powered-up, it has no knowledge of which cell it belongs to, which frequencies or bandwidth to use. This means that the first thing a terminal must do is to acquire this kind of information. This is done in the following steps:

- Frequency and symbol synchronization to a cell.

- Frame timing of the cell.

- Finding the cell identity of the cell.

To aid the terminal in finding the cell identity, there are two reference signals, *Primary Synchronization Signal* (PSS) and *Secondary Synchronization Signal* (SSS). Each of these signals occur twice per frame and the time-domain location depends on whether the eNodeB is operating in FDD or TDD. The two PSS within a frame are identical while the two SSS differ. The reason for SSS_1 and SSS_2 differing is to allow the UE to obtain frame timing.

There are 504 different *physical-layer cell identities* [3, Ch. 6.11], which are further grouped into 168 *cell-identity groups*.

PSS & SSS

Once the PSS has been found, the terminal has a five millisecond timing of the cell. Since the SSS has a fixed location relative the PSS, the location of the SSS is also known. In addition to that, once the PSS has been identified, the cell identity within the cell-identity group is known, since the PSS can take only three values corresponding to the cell identity within the cell-identity group. The cell-identity group itself is not known until the SSS is identified. Thus, identifying both the PSS and SSS is enough to find the physical-layer cell identity. By knowing the locations of the PSS and SSS within a frame, the terminal knows the frame timing and has then identified the cell-specific reference signal, needed for the decoding of system information within the cell. The PSS is based on Zadoff-Chu [13] sequences while the SSS is based on m-sequences[19].

With the cell-specific reference signal known, the terminal can decode the system information which is repeatedly broadcasted by the network. The system information is needed to get access to the network.

MIB & SIB

The system information is divided in two different types; *Master-Information Block* (MIB) and *System-Information Block* (SIB), and are broadcasted on different transport channels. The MIB is broadcasted on the BCH and contains some general information about the cell, such as the downlink cell bandwidth and the SFN. The MIB uses a shorter CRC of 16-bits instead of the normal 24-bits to keep the overhead down. It uses a rate-1/3 tail-biting convolutional code as opposed to Turbo codes in all the other downlink transport channels because it simply outperforms Turbo codes for such small blocks.

The MIB is sent over 72 subcarriers, which conveniently is the minimum possible bandwidth in the downlink. The terminal can then assume a bandwidth of six resource blocks until it has found the actual bandwidth for the cell, which can only be equal to or higher than 72 subcarriers. Each BCH transport block is mapped to the first subframe of each frame in four consecutive frames. It is thus transmitted every 40 ms. The extensive amounts of repetition might seem like a waste of resources, but one should keep in mind that the MIB should be able to be decoded by the terminals within the cell as well as terminals in neighboring cells. Since the interference might be high in neighboring cells, the extra processing gain from repetition is needed. For terminals with high *signal to interference and*

noise ratio (SINR), only a few of the subframes might be needed, as it could be sufficient for correct decoding.

The SIB is broadcasted on the DL-SCH and contains more information than the MIB. To keep track on which information on the DL-SCH being system information, the PDCCH is marked with a *System Information Radio Network Temporary Identifier* (SI-RNTI). There are 13 different SIBs defined, where each SIB is characterized by the type of information in them. SIB-1 for instance, contains among other things information on where to find the rest of the SIBs. SIB-2 is of interest in the next section as it indicates which time-frequency resources are available for random access preamble transmission. Generally, SIBs with lower numbers occur more frequently. More information about the SIBs can be found in [8]

2.4.2   Random Access

To get access to the network, the terminal must request a connection setup, which is commonly referred to as *random access*. In LTE, the random access can be used for several reasons. Those which are of interest for this thesis are presented in the list below:

- Initial access when establishing a radio link.

- Re-establish a radio link after radio link failure.

- Establishing uplink synchronization when in RRC_CONNECTED, but not uplink synchronized.

- Requesting scheduling if no dedicated scheduling-request resources have been configured on the PUCCH.

In the contention based random access procedure, there are four steps. If any of the steps were to fail, the terminal would have to restart the attempt from step one. The steps are presented in the next four subsections.

1. Random-Access Preamble Transmission

In the first step, the terminal chooses a random access preamble (described in Section 2.5) at random and transmits it to the eNodeB. The random access preamble must be sent only on the PRACH and its purpose is to indicate to the eNodeB that a random access attempt is being performed as well as for timing information. When the eNodeB receives the preamble, it estimates the delay and in the second step it sends timing adjustments back to the terminal.

If no two terminals within a cell transmit the same preamble at the same random access resource, no collision occurs and the eNodeB might be able to recognize the preamble, depending on the SINR of the preamble. If two or more terminals transmit different preambles, the eNodeB is able to detect them as long as the interference between the preambles is not too high. Since Zadoff-Chu sequences are used, the correlation between the different preambles is quite low, thus reducing the interference between preambles.

In FDD, there is at most one random access region per subframe, that is, several regions cannot be spread in frequency. The timing varies between once per ms to once per 20 ms. In TDD, it is possible to combine several random access regions in frequency and they can occur up to six times per 10 ms.

2. Random-Access Response

In the second step, the eNodeB will transmit a random-access response on the DL-SCH. The content of the message is:

- The indices of the preambles received.

- Timing corrections.

- Scheduling grants on the UL-SCH.

- Temporary identifiers, *Temporary Cell Radio-Network Temporary Identifier* (TC-RNTI).

The indices of the preambles are transmitted so that the terminals will know whether their preamble were received correctly or not. The timing corrections are necessary for further communication with correct timing. The scheduling grant on the UL-SCH is necessary since it otherwise has no permission to use the uplink data channel. The temporary identifier will be used in the next steps until it has received a *Cell RNTI* (C-RNTI).

The presence of the Random-Access response in the DL-SCH is indicated in the PDCCH, which the terminals who have sent a preamble will monitor. In case several terminals sent preambles, a response is sent to each of the requests which were correctly identified. In case several terminals used the same preamble, a collision will occur. The random-access response will still be sent as it is difficult for the eNodeB to determine how many terminals a certain preamble corresponds to. Since different terminals should have different timing adjustments, some terminals might receive a response intended for others, which could lead to those terminals disturbing other users on the UL-SCH when they transmit with incorrect timing. These conflicts will be dealt with in the next steps.

3. Terminal Identification

In the third step, the terminal sends its C-RNTI along with some additional information depending on the state of the terminal. The transmission is done on the UL-SCH which is beneficial in several ways. The amount of information sent on the random-access channel should be minimized since no uplink synchronization leads to a lot of waste because of the large guard periods. In UL-SCH, the terminal can also adjust modulation more dynamically depending on the state of the channel. When transmitting on the UL-SCH, hybrid ARQ with soft combining is possible, which means that if retransmission must be made, the energy from the previous transmissions can be used to make more accurate decisions.

If the terminal already has a cell context, that is being RRC_CONNECTED, the terminal sends its C-RNTI as previously described. If not, a core-network termi-

nal identifier is used which means that some processing between the eNodeB and the core network prior to the eNodeBs response in the fourth step is needed.

4. Contention Resolution

In the fourth step, the downlink message contains information on contention resolution. The message contains the identifiers from the previous steps which the terminals can compare with to see who succeeded in the random-access procedure. For those terminals having used a temporary identifier, the message will also contain a C-RNTI which will replace the temporary one. The message is sent on the DL-SCH and hybrid-ARQ is used, which means that the terminal will have to send hybrid-ARQ ACKs.

By responding to only certain terminals with their corresponding identifiers, the other terminals whose preamble collided will not find a match and will consider the random-access process failed and will retry from step one. In case a terminal does not find the message from step four within a certain time, it will consider the random-access procedure failed.

After the fourth step, some RRC-reconfiguration might occur.

2.4.3   UE Initiated Uplink Transmission

When the terminal has a C-RNTI and a radio link is established with uplink synchronization, the transmission of the intended data can be done. If the terminal has received a scheduling on the PUCCH, it will use it to request an uplink grant so that it can transmit the data on the PUSCH. If it has not, it will request an uplink scheduling grant through a random access procedure.

2.5   Random Access Preamble

This section gives details on the random access preamble used in the uplink in the first step of the random access procedure.

As mentioned in the previous section, the first step of the random-access procedure, is the transmission of a random access preamble. The RA-preamble is a signal which is roughly 6 RB wide in frequency and normally 1 ms in time. Each cell has a set of 64 preambles which are generated from Zadoff-Chu sequences. The reason for using Zadoff-Chu sequences is for their desired correlation properties, where the correlation between different root sequences and their cyclic shifts are very low. For further details on Zadoff-Chu sequences, please refer to [13]. In the time domain the preamble is defined as [3, p. 44]:

$$s(t) = \beta_{\text{PRACH}} \sum_{k=0}^{N_{\text{ZC}}-1} \sum_{n=0}^{N_{ZC}-1} x_{u,v}(n) e^{-j\frac{2\pi nk}{N_{ZC}}} e^{j2\pi(k+K)\Delta f_{\text{RA}}(t-T_{\text{CP}})} \qquad (2.2)$$

where $0 \leq t < T_{\text{SEQ}} + T_{\text{CP}}$. β_{PRACH} is an amplitude scaling factor, K is a constant

defined in [3, p. 44], N_{ZC} is the length of the Zadoff-Chu sequence and $\Delta f_{\text{RA}} = 1250$ Hz, is the preamble carrier spacing.

The uth root Zadoff-Chu sequence is defined as:

$$x_u(n) = e^{-j\frac{\pi u n(n+1)}{N_{\text{ZC}}}}, 0 \leq n \leq N_{ZC} - 1 \tag{2.3}$$

and $x_{u,v}(n)$ are different cyclic shifts of the uth root sequence according to [3, p. 40].

Table 2.1 shows the different sequence lengths specified. The N_{ZC} value of interest in this thesis are those used in preamble format 0–3, that is $N_{ZC} = 839$. The reason for choosing the higher value is because the preamble format 4 is transmitted during a relatively short time, leading to less accumulated energy than in the case of preamble format 0–3.

Preamble format	N_{ZC}
0-3	839
4	139

Table 2.1: Random access preamble sequence length.

As can be noted from the preamble definition (2.2), the preamble occupies roughly $839 \cdot 1250$ Hz ≈ 1.05 MHz, which is about 30 KHz less than 6 RB.

The length of the preamble sequence, T_{SEQ}, and the cyclic prefix, T_{CP}, depends on the preamble format as shown in table 2.2

Preamble format	T_{CP}	T_{SEQ}
0	$3168 \cdot T_{\text{s}}$	$24576 \cdot T_{\text{s}}$
1	$21024 \cdot T_{\text{s}}$	$24576 \cdot T_{\text{s}}$
2	$6240 \cdot T_{\text{s}}$	$2 \cdot 24576 \cdot T_{\text{s}}$
3	$21024 \cdot T_{\text{s}}$	$2 \cdot 24576 \cdot T_{\text{s}}$

Table 2.2: Sequence and cyclic prefix length for some preamble formats.

As T_{s} is defined as $1/(15000 \cdot 2048)$ s, the preamble format 0 corresponds to a total duration of 1 ms, where the cyclic prefix occupies approximately 0.1 ms, the sequence 0.8 ms, which leaves 0.1 ms for guard period, which is necessary because of timing uncertainty. In the case of the preamble format 3, the whole duration is 3 ms where 0.72 ms is guard period. It is thus possible to pick different lengths depending on the desired robustness against timing uncertainty. With the signal traveling in the speed of light, $c = 3 \cdot 10^8$ m/s, the uplink timing uncertainty becomes 6.7 µs/km. For the preamble format 0, this allows for cell sizes up to approximately 15 km, while preamble format 3 theoretically allows cell sizes of over 100 km (if the SNR is high enough is another problem).

3

Extended Coverage

In this chapter, some alternatives for extended coverage are discussed. Energy accumulation is considered the main option and is the method the proposed improvements are based on.

3.1 Ways of Improving SNR

There are many ways of improving the SNR for a user terminal/eNodeB. In this section, the alternatives listed below are discussed:

- Multi-antenna techniques
- Power boosting
- Coordination
- Repetition

3.1.1 Multi-Antenna Techniques

Multiple-Input Multiple-Output MIMO refers to the use of multiple antennas at both the receiver and transmitter and has several advantages such as improved data rate, improved reliability and reduced interference. When having several antennas at both the receiver and transmitter, it is possible to transmit data in several independent streams, although this is not of interest in the case of low SNR as in this thesis.

By having several antennas, sufficiently separated from each other, they can be viewed as independent channels which can be used to combat fading effects.

Lately, the interest of massive MIMO has increased and it is a good candidate for a new mobile standard.

Even though MIMO is promising in many ways, it is not possible to use many of the advantages before having some channel information and information about the location of the transmitter/receiver. Since that sort of information is not possible for a terminal before connection setup, none of the advantages of MIMO can be used in the early steps.

Another way of increasing the antenna gain is to use higher order sectorization. Normally, a site consists of three antennas, where each antenna spans an angle of 120°. By decreasing the angle for each antenna, the antennas can focus the energy within a smaller angle and increase the SNR. Since the antennas focus on a more narrow area, more antennas are required for a 360° coverage. Installing additional antennas comes with large costs, implying that other ways of improving SNR have to be considered.

3.1.2   Power Boosting

A quite obvious candidate for improved SNR is power boosting, which means to increase the transmit power. In the case of uplink, most terminals with bad radio conditions are already using full power, but in the case of downlink this is possible.

In both uplink and downlink, it is possible to concentrate the energy in the frequency domain. By using the same power for e.g. half the bandwidth, 3 dB is gained.

Another power boosting aspect is the power tradeoff between data and demodulation/reference signals. By concentrating more of the power on the reference signals, the channel estimation improves, possibly resulting in a total positive gain in the demodulation. That is of course only applicable where such reference signals are used, e.g. in the data channels.

3.1.3   Coordination

One set of alternatives when it comes to coordination options is *Coordinated Multi-Point transmission and reception* (CoMP). Basically, the aim of all CoMP techniques is to dynamically coordinate the transmission and reception of several geographically separated antennas. One example is a terminal on a cell edge, where the nearby eNodeBs combine their received signals from the terminal to make a more accurate decision. Reversely, the eNodeBs could also coordinate the transmission to the terminal, which will both lead to more received power and increase the ability of reducing interference.

Since release 9, *Multicast-Broadcast Single-Frequency Network* (MBSFN) has been possible in LTE. By sending the information from several cell sites, the signal appear at the receiver as if it has been subject to multipath propagation. Because of OFDMs robustness against multipath propagation, the signal will both become stronger and reduce the interference.

3.1.4 Repetition

The previous options are capable of increasing the SNR a few extra dB, but the costs are relatively high compared to the actual gain due to hardware costs and increased complexity. The main option to be considered in this thesis is energy accumulation. It simply means that the signals are repeated over a longer time, which also gives some time diversity.

The cost of repetition is mainly lower data rate and higher latency, which is something MTC-devices generally can tolerate to a relatively high extent compared to human centric UEs. The repetition option needs only software upgrades at the eNodeB, thus avoiding expensive hardware upgrades on the network side.

3.2 Proposed Improvements

This section presents some rough ideas for implementation in the LTE standard. In Chapter 4, the idea of energy accumulation is further elaborated and the simulations to evaluate the proposed methods are presented along with discussions of the results. The concepts and pictures from this section comes from internal Ericsson documents.

When it comes to energy accumulation, there are two aspects which are of main interest in the pursuit of increasing the effective SNR and counter the effect of Rayleigh fading. These are *coherent* and *non-coherent* accumulation. Because of channel variations over time, it is not possible to coherently accumulate a signal for any duration. The time over which a channel is considered to be constant is called the *coherence time* and is denoted T_d. The time over which coherent accumulation is possible is therefore the coherence time. To accumulate sections which are non-coherent to one another, a less efficient accumulation method in terms of SNR gain will be used.

The quality of the channel for two non-coherent segments is assumed to be independent, which allows for some time diversity. In this thesis report, the number of coherent and non-coherent accumulations will be denoted N_c and N_nc respectively. The exact modeling of how N_c and N_nc will affect the signal will be discussed in Chapter 4.

The bottom of the bars in Figure 3.1 corresponds to the link budget for some channels and the top is the targeted link budget improvement. The data rate of the PUSCH and PDSCH is 20 kbps. The link budget improvement target for some channels is showed in Table 3.1 [12]. As can be seen, the most challenging channels are the PRACH and the PUSCH. In the case of data channels, some dB improvement of the effective SNR can be achieved by reducing the bit rate[1]. This is quite a flexible way of improving the SNR as compared to the case of the PSS/SSS and the PRACH. Since they do not transmit bits, the bit rate cannot be

---

[1]This comes from the fact that accumulating two coherent repetitions of the same signal results in a factor 2 increase of the amplitude but only a factor 2 increase of the noise variance.

lowered, but instead, all the increase of SNR must come from other improvement methods, such as those discussed in Section 3.1.

Physical channel name	Coverage improvement target [dB]
PUCCH(1A)	13.5
PRACH	19.0
PUSCH	20.0
PDSCH	15.3
PBCH	11.7
SCH	11.4
PDCCH(1A)	14.6

Table 3.1: Coverage improvement targets for some channels (FDD).
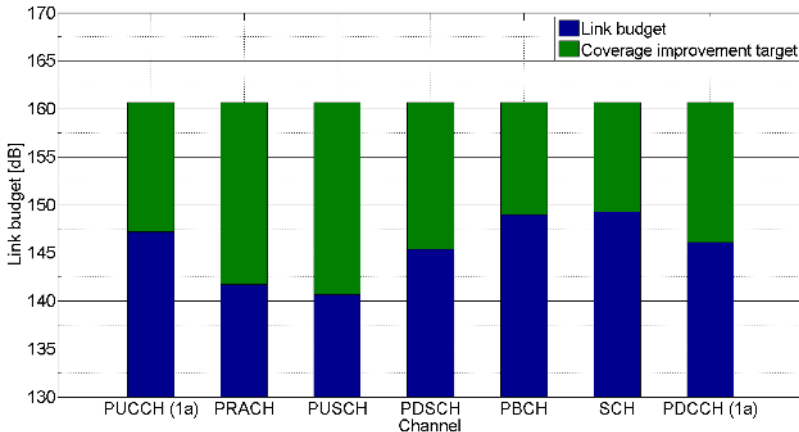
Figure 3.1: Link budget and improvement targets for some LTE channels

Instead of making major changes to the existing channels, causing problems for legacy users, the idea is to create new overlay channels. The new channels will be put in the data region, thus allowing backwards compatibility. It also allows for e.g. simpler protocol solutions by having fewer control channels and/or by having a single ARQ level with fixed transport block size, to simplify the energy accumulation.

The overlay channel components and their functionalities are presented in the list below.

- The *Synch channel* substitutes the functionality of the PSS/SSS.

- The *Access SIB* substitutes the normal MIB and SIB and contains only limited information related to initial system access.

- The overlay data channels substitute the downlink and uplink shared channels and control channels.

- The overlay RACH will substitute the normal RACH and will exist in different sizes designed for the coverage limited terminals.

3.2.1 Inband Overlay

It is assumed that the users who can find the normal PSS/SSS and decode the normal MIB & SIB will do so and are thereby not considered coverage limited. In the case of coverage limited users, a more robust procedure must be used, and one idea is to use a special access SIB with system information for coverage limited users. Since much of the information contained in the normal SIB are not needed for the group of coverage limited MTC-devices, the access SIB can contain less information compared to the normal SIB. To not interfere with the normal PSS/SSS, all the overlay channels avoids certain subframes in the data region, such as subframe 0 and 5 in the case of FDD.
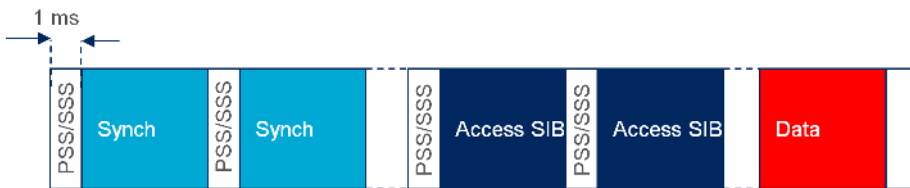
Figure 3.2: *Illustration of the scheduling of the Synchronization channel, Access SIB and Data channels*

One might think that the quantity of periodically broadcasted data, such as synchronisation and access SIB will be immense, leading to an extreme overhead, occupying a great amount of resources. By having MTC-devices with low requirements on latency and data rate, the signals can occur less frequent, allowing the overall overhead to be kept at corresponding level to the normal information which is broadcasted. An example can be seen in Figure 3.3, where the length of the synch is 10ms and the access SIB 100ms.
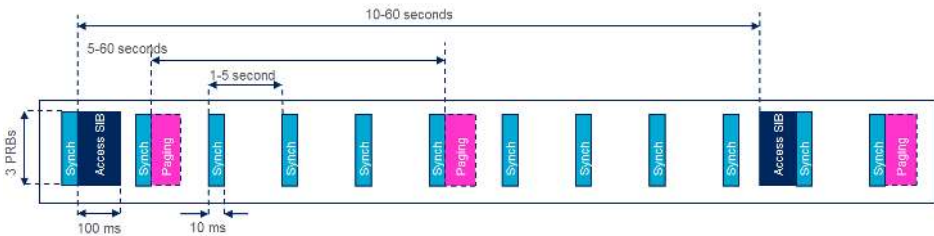
Figure 3.3: *Illustration of the periodicity of the synchronization channel and access SIB*

In the case of having a synch periodicity of 1 s and an access SIB every 10 s, the overhead will be $0.01/1 + 0.1/10 = 2\%$, meaning that the overhead of synch and access SIB will be less than or equal to 2% with the settings according to Figure 3.3.

3.2.2   RACH

The normal RACH does not suffice for the coverage limited MTC-devices, which means that the overlay RACH must be adjusted accordingly. Normal RACH uses power control which is simply not enough in the case of extreme coverage limitation, so in the robust procedure, time control is used.

The location of coverage limited MTC-devices is assumed to be uniformly distributed, resulting in different users having different repetition needs. In the ideal case, each terminal would be provided with the exact amount of repetition needed for a desired SNR. In practice, such flexible choice of repetition will not be practical in the RACH for several reasons. The terminal would need to have the exact knowledge on how much repetition it requires and the chosen repetition would have to be communicated between the terminal and the eNodeB, which would not be feasible before the first random access attempt. In addition to that, such signalling would also have to be repeated.

One idea for providing appropriate random access resources to the users is to create a number of fixed RACH-sizes. An example is having lengths of 10 ms, 20 ms, 40 ms, 80 ms, 160 ms. The terminals chooses the duration needed depending on the received power in the downlink. Since the user group aimed in this thesis typically do not need to transmit data continuously, these extra RACH resources could be scheduled at certain time instances declared in the access SIB, with a periodicity adjusted according to the number of coverage limited MTC-devices.

Figure 3.4: *Illustration of different RACH sizes*

In the design of the overlay channels, it is important to design suitable sizes according to the need of the users. Too large differences in repetition length might lead to a waste of resources while too many choices of repetition length might imply unnecessary control signaling. This thesis does not aim to find a balance of these parameters nor to design higher layer aspects, but instead, assumes a basic overlay channel setup and focuses on the physical layer aspects which are presented in the next chapter.

4

Simulations & Numerical Results

To examine how well the proposed methods for extended coverage work, simulations are needed. The simulations in this thesis provide the magnitude of the data-rate for different situations. The simulations are divided into three parts. The first part evaluates the PRACH, the second the SNR distribution in downlink and the third part the PUSCH.

4.1   PRACH Simulation

As stated in the introduction, this thesis focuses on coverage limited MTC-devices and their performance for low-data rate applications. The coverage limitation is assumed to mainly depend on how deep inside of a building the devices are located and the distance from the strongest base station. Some MTC-devices might be located outdoors and have excellent coverage, which means that they have no need for an increase of SNR, thus being out of scope for this thesis. Others might be located indoor or outdoor, close to the cell edge, where an increase of SNR is needed.

The coverage limitation occurring because of the penetration through an exterior wall is modeled by 3GPP [10, p. 55] as an additional path loss of 20 dB. The MTC-devices are in this thesis modeled as having an indoor loss uniformly distributed in the interval [20,40], which means that the worst case users will have a 40 db indoor loss. This is supposed to represent the case where an MTC-device is placed deeper indoor. For convenience, four different user cases are defined and referenced to in this thesis. The definitions are defined in Table 4.1 where the additional path loss refers to the path losses due to indoor losses.

The bad indoor case is the main model used for the MTC-devices and means that

User case	Additional path loss [dB]
Outdoor	0
Indoor	20
Bad indoor	[20,40]
Worst indoor	40

Table 4.1: Random access preamble sequence length

the additional path loss is uniformly distributed in the interval $[20, 40]$.

One might think that the channels frequency characteristics are constant, since both the MTC-device and eNodeB are stationary, but this is typically not the case. Objects located between a terminal and eNodeB, for example vehicles, might be moving, thus affecting the different paths, as shown in Figure 4.1.
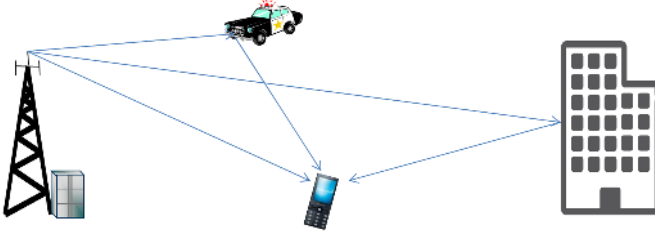
Figure 4.1: Illustration of a radio link with reflections.

4.1.1 Channel Model

The signal from the different paths will arrive at the receiver at different time instances, which means that a number of differently delayed signals with different phase shift are being superpositioned. Thus, if $x(t)$ is the transmitted base-band signal, the received signal will be [20]

$$y(t) = \sum_{k=1}^{M} A_k e^{j\phi_k - j2\pi f_c \tau_k} x(t - \tau_k),$$

where k is the index of the kth path, A_k is the amplitude, ϕ_k is the phase difference, τ_k is the relative delay which also causes additional phase lag in the last exponent. Since LTE operates in higher frequencies, in the order GHz, the phase lag $2\pi f_c \tau_k$ modulo 2π can be considered a random phase, uniformly distributed in the interval $[0, 2\pi]$. The total phase shift $\theta_k = \phi_k - 2\pi f_c \tau_k$ can therefore also be considered a random variable, uniformly distributed in the same interval, $[0, 2\pi]$. The channel's impulse response can then be written as:

$$h(t) = \sum_{k=1}^{M} A_k e^{j\theta_k} \delta(t - \tau_k).$$

The Fourier transform then becomes

$$H(f) = \sum_{k=1}^{M} A_k e^{j\theta_k} e^{-j2\pi f \tau_k}.$$

For a small frequency band around f_0, the channel can be modeled as a scalar gain [20]

$$h \approx H(f_0) = \sum_{k=1}^{M} A_k e^{j\gamma_k},$$

where $\gamma_k = \theta_k - 2\pi f \tau_k \bmod 2\pi$.

Based on the central limit theory, it can be shown [20] that for large values of M, the channel h is proper complex Gaussian

$$h \sim CN \left(0, \sum_k A_k^2 \right). \tag{4.1}$$

Since h is modeled as small-scale Rayleigh fading, it is normalized so that $E[h \cdot h^*] = 1$. The channel is therefor modeled as a complex normal Gaussian variable with variance 1; $h \sim CN(0, 1)$.

In reality, there are many paths arriving at a receiver, thus making a Rayleigh faded channel a valid channel model for the scenarios in this thesis.

4.1.2 Preamble Detection Link Simulation Setup

In the case of the transmission of the preamble in the random-access procedure, it is of interest to know the probabilities of a miss/false detection for different SNR values. To find this out, the link simulation have been set to the constellation of the preamble as described in Section 2.5 in terms of bandwidth. The gain compared to today's LTE comes from the coherent and non-coherent accumulation.

Section A.1 goes into details on how the signals have been modeled.

By simulating the ability to detect the preamble for different values of N_c and N_{nc} for different SNRs, knowledge on how the signal needs to be strengthened is gained. Questions such as how much should be put on coherent accumulation

and how much should be put on non-coherent accumulation (time diversity or frequency hopping), given some amount of repetition available ($N_c \cdot N_{nc}$), will be answered with the link simulations.

For pseudo code of the link simulation please refer to section A.2.

4.1.3 Link Simulation Results

This section covers the results from the link simulation of the PRACH. It is of interest to see the results of the link simulations when iterating over different values for N_c and N_{nc} to see the effect of coherent accumulation and time diversity. The following figures shows the results from

$$N_c \in \{1, 2, 4, 8\}, \text{and}$$

$$N_{nc} \in \{1, 2, 4, 8, 16, 32, 64\}.$$

Each figure corresponds to a fixed N_c-value for different N_{nc}-values, where the maximum repetition is 128. This means that the available repetition will be powers of two up to 128, that is, $N_c \cdot N_{nc} \leq 128$. The number of coherent accumulations is limited to 8 due to limitations from the coherence time.

The receiver (eNodeB) is assumed to have two uncorrelated antennas, leading to additional diversity, which means that the effective value of N_{nc} will be twice as much as the actual non-coherent repetition.

The results are presented in Figure 4.2–4.5.
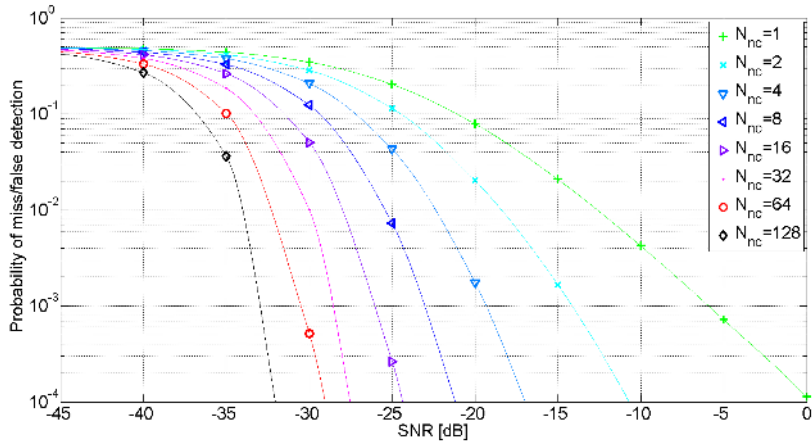
Figure 4.2: *Probability of miss/false detection with $N_c = 1$.*
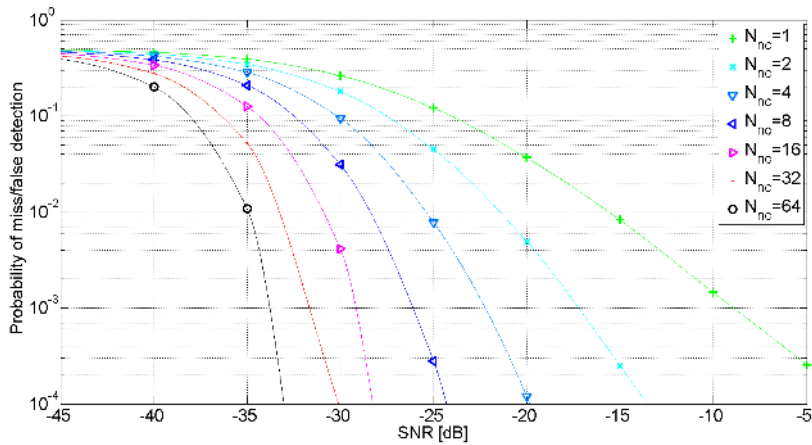
Figure 4.3: *Probability of miss/false detection with $N_c = 2$.*
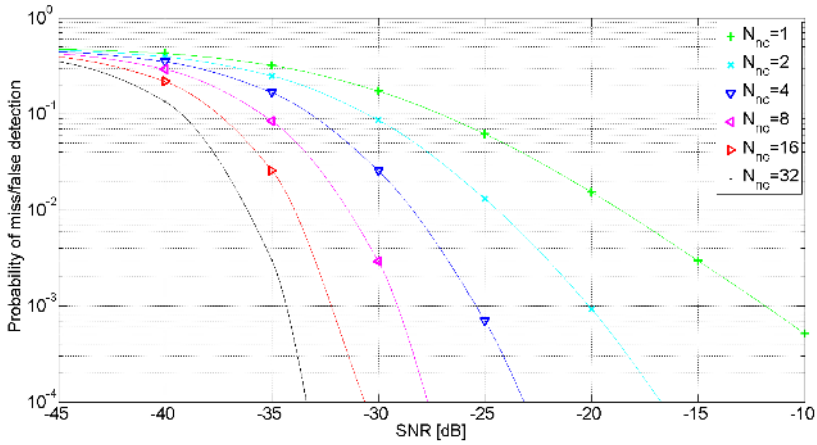
Figure 4.4: *Probability of miss/false detection with $N_c = 4$.*
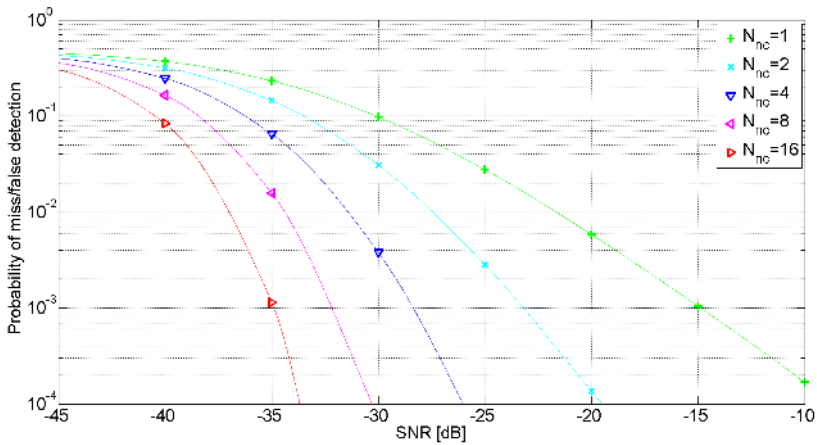
Figure 4.5: *Probability of miss/false detection with $N_c = 8$.*

As can be seen in the Figure 4.2–4.5, the signal gets a slight shift to lower dBs with coherent accumulation while the non-coherent accumulation gives rise for steeper curves. The reason for this is that the non-coherent accumulation involves energy accumulation from different time instances with independent channels which partly battle fading effects. If the channel were a simple AWGN channel, the coherent would be the best choice.

From a terminal point of view, it is important so select the combination of repetition which results in the lowest error probability, given a SNR and a probability. As the probability for miss/false detection in the case of preamble detection is aimed to be 10% or less, the best combinations of repetition can be chosen with the constraint that coherent accumulation can be done for a maximum of 8 ms. In the case of preamble transmission, the repetition scheme chosen and its performance is showed in Figure 4.6.
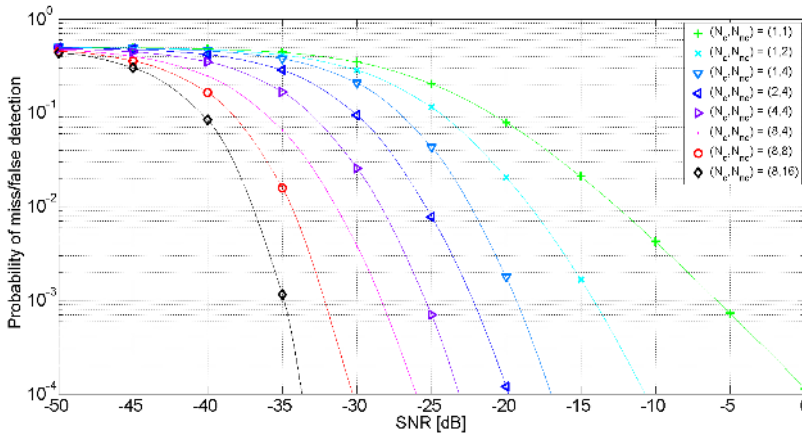
Figure 4.6: *Repetition scheme for random access preamble.*

4.1.4 System Simulation

For the evaluation on system level, a system simulator developed at Ericsson Research has been used. The propagation model used is the widely known Okumura-Hata model [11, p. 85–86], which is completely based on empirical data measured in Tokyo in the frequency range 200 MHz–2 GHz. It is divided into three categories, open areas, suburban areas and urban areas. In the simulations made in this thesis, the urban category has been used.

In the system simulation the area is divided into a hexagonal grid, as shown in Figure 4.7, where each base station has three cells (hexagons). The *inter-site distances* (ISD) used in the simulations are 500 m, 1732 m, 2500 m and 5000 m. To simulate large areas, wrap around has been used. It means that a limited number of hexagons makes up a limited area, in this case 7 sites, 21 cells, and the area outside is simply the base area repeated so that signals going out on one side

of the 7 sites, will simply turn up on the other side. This allows for interference from nearby sites to be taken into account.
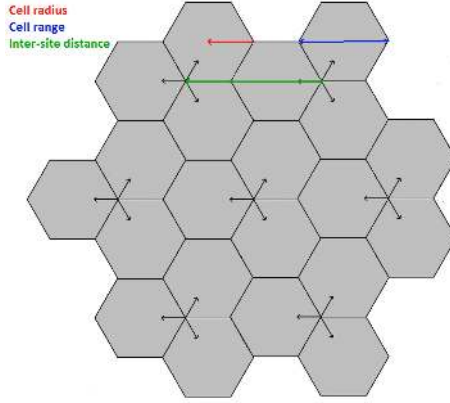
Figure 4.7: *Deployment of base stations/sites according to a hexagonal pattern where each hexagon corresponds to one cell. Each site consists of three cells.*

Since the MTC-devices considered in this study have a fixed location, the distance between the eNodeB and terminal could be considered constant. However, because of the reasons mentioned in the beginning of this chapter, the terminal is not modeled with a static channel. Because of variations of the channel, the non-moving terminals in this thesis are modeled as having a multipath speed of 0.15 m/s.

The system simulation aims to find out the CDF of the distribution of the users SNR in uplink. The SNR in the uplink is defined as

$$\text{SNR} = \frac{P_{\text{UE}} \cdot g_{\text{max}}}{N_{\text{ul}}}, \tag{4.2}$$

where P_{UE} is the power of the UE, N_{ul} is the thermal noise in uplink, and g_{max} is the maximum path gain.

When looking at the SNR, it is of interest to put the results in relation to the results of other types of users. The user cases of interest are outdoor, indoor, bad indoor and worst case indoor.

Figures 4.8 - 4.11 show the results of the SNR in uplink for the four inter-site distances used and Figure 4.12 shows all the inter-site distances plotted against each other for the bad indoor case. The output power is assumed to be 0.2 W [9] over the bandwidth 1.05 MHz and the uplink noise figure, F_{ul}, is set to 5 dB. The figures show the distribution of the users SNR. Note that fast fading effects has not been taken into account.
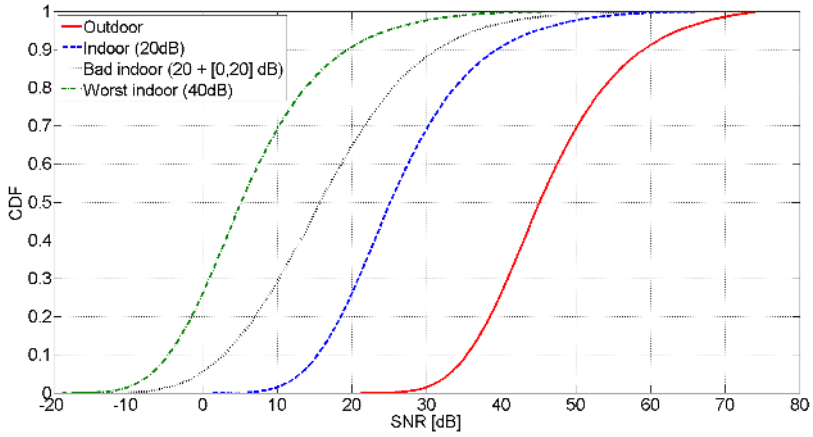
Figure 4.8: *CDF-plot of the SNR in uplink for inter-site distance 500 m.*
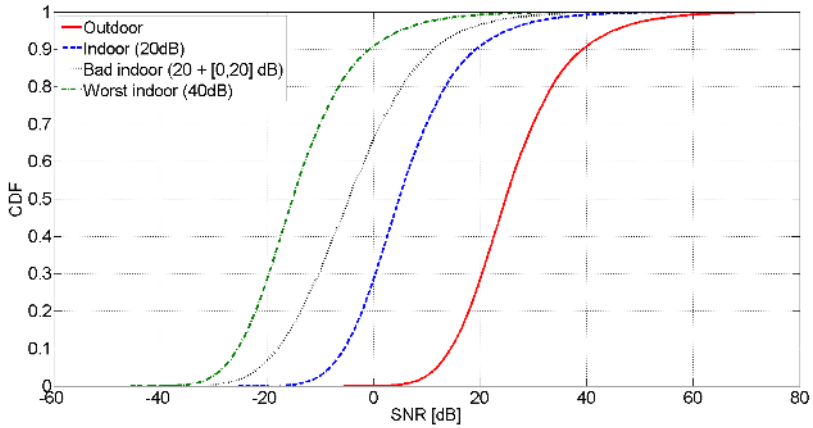
Figure 4.9: *CDF-plot of the SNR in uplink for inter-site distance 1732 m.*
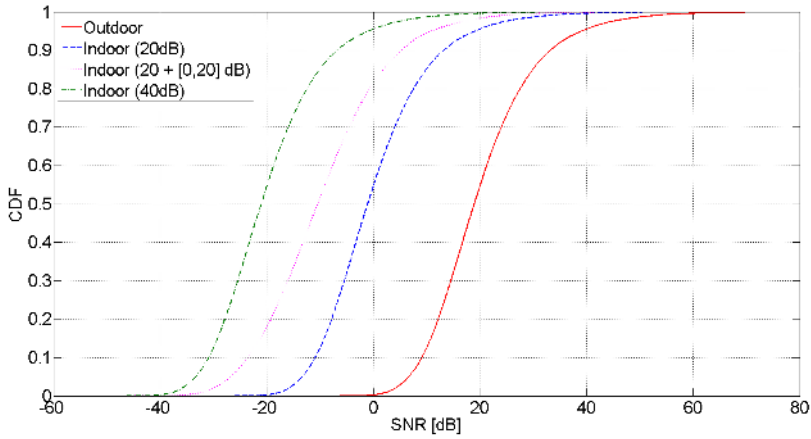
Figure 4.10: *CDF-plot of the SNR in uplink for inter-site distance 2500 m.*
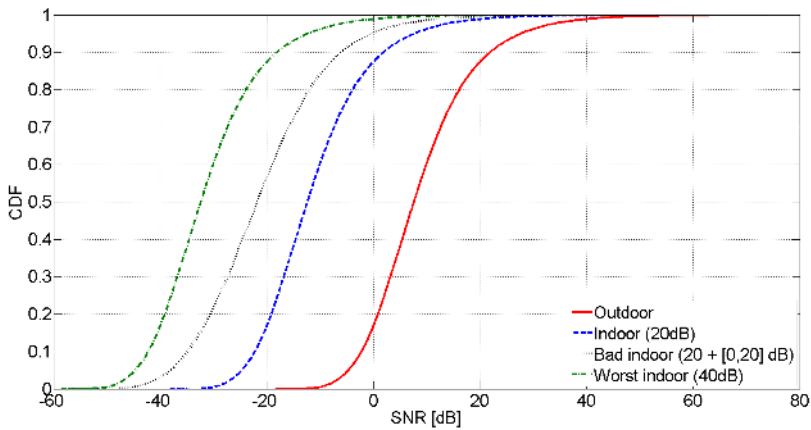
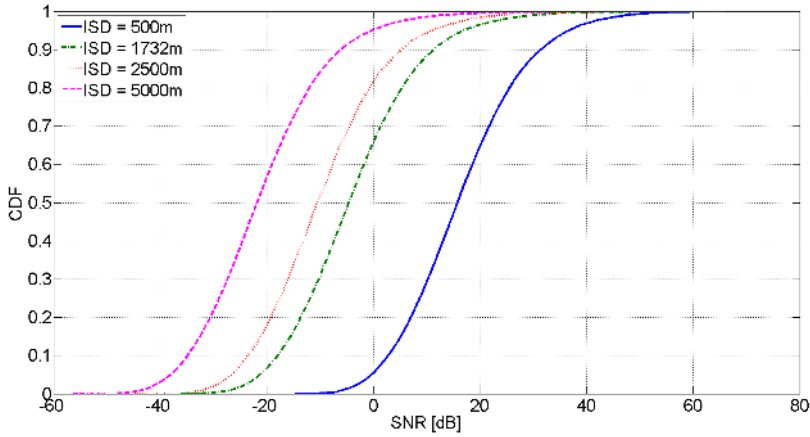**Figure 4.11:** *CDF-plot of the SNR in uplink for inter-site distance 5000 m.*

Figure 4.12: *CDF-plot of the SNR in uplink for different inter-site distances for the bad indoor case.*

As can be seen in the figures, there are a lot of similarities between the different type of users in all the inter-site distance cases. The big difference is the whole CDF being shifted to the left for longer inter-site distances. The shape of the CDF-curve is similar in all the cases which can be seen in Figure 4.12. Since the interference is not considered in the SNR-plots, the important factors are the locations of the users and their random extra path loss.

4.1.5   Random Access Preamble

The combination of the uplink SNR plots and the result from the link simulations will result in statistics of how much repetition is needed for the random access preamble, given a certain set of users. In the case of the random access preamble transmission, the acceptable probability for a miss/false detection, $p_{\text{miss/falsedetection}}^{\max}$ is set to 10%. Each user will, if possible, use the smallest possible set of repetition which results in a probability which is equal to or less than $p_{\text{miss/falsedetection}}^{\max}$. If that is not possible, the user will use the maximum repetition scheme.

For each user with a certain $p_{\text{miss/falsedetection}}^{\max}$ and repetition $N_c \cdot N_{nc}$, the average number of preambles used for user k is

$$R_k = \lim_{i \to \infty} N_{\text{c}}^{(k)} N_{\text{nc}}^{(k)} (1 - p_k) + 2 N_{\text{c}}^{(k)} N_{\text{nc}}^{(k)} (1 - p_k) p_k + \ldots + (i+1) N_{\text{c}}^{(k)} N_{\text{nc}}^{(k)} (1 - p_k) p_k{}^i.$$

p_k is the probability of a miss/false detection for user k. This expression results in

$$R_k = N_c^{(k)} N_{nc}^{(k)} (1 - p_k) \sum_{i=0}^{\infty} (i + 1) {p_k}^i = \frac{N_c^{(k)} N_{nc}^{(k)}}{(1 - p_k)}. \tag{4.3}$$

If R_k is calculated for all the users of interest, the total average of the users will be $R_{\text{average}} = \frac{\sum_{k=i}^{N} R_k}{N}$, where N is the number of users of interest. The algorithm for making these calculations is further elaborated in Section A.3.

Figures 4.13 - 4.15 show the repetition distribution of the users for the case $p_{\text{miss/falsedetection}}^{\text{max}} = 10\%$, for the three longest inter-site distances. The repetition schemes used are those specified in Figure 4.6 with the bad indoor case.
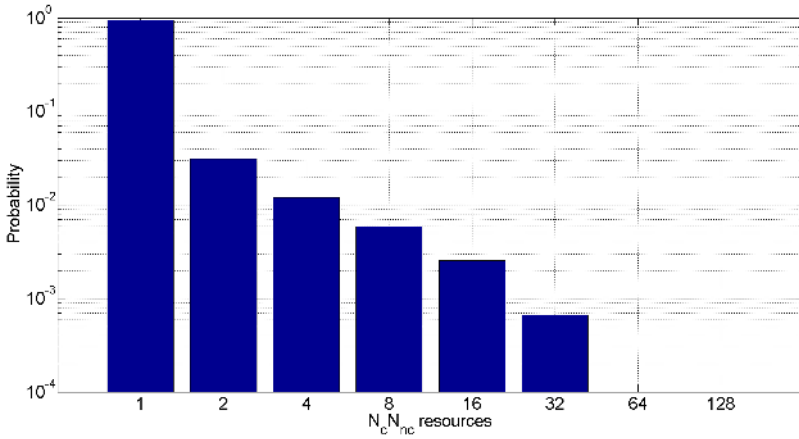
Figure 4.13: *Distribution of repetitions for users with the bad indoor case in cells with inter-site distance 1732 m*

The reason the inter-site distance 500 m has not been plotted is because no users need any repetition in that case for the specified value of $p_{\text{miss/falsedetection}}^{\text{max}}$.

As expected, the number of users using more repetitions increases with longer inter-site distances. In the longest case, the available repetition is saturated and the worst case users end up with a probability of missing/misdetecting a preamble larger than $p_{\text{miss/falsedetection}}^{\text{max}}$. The resulting average number of preambles needed is presented in Table 4.2.

4.2 Downlink Simulation

In the downlink, the geometry, which is a measure of signal to noise interference, is of interest, which here is defined as
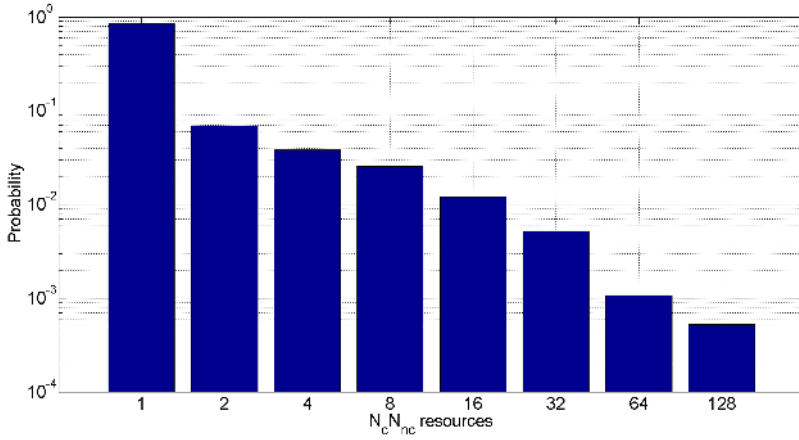
Figure 4.14: *Distribution of repetitions for users with the bad indoor case in cells with inter-site distance 2500 m*
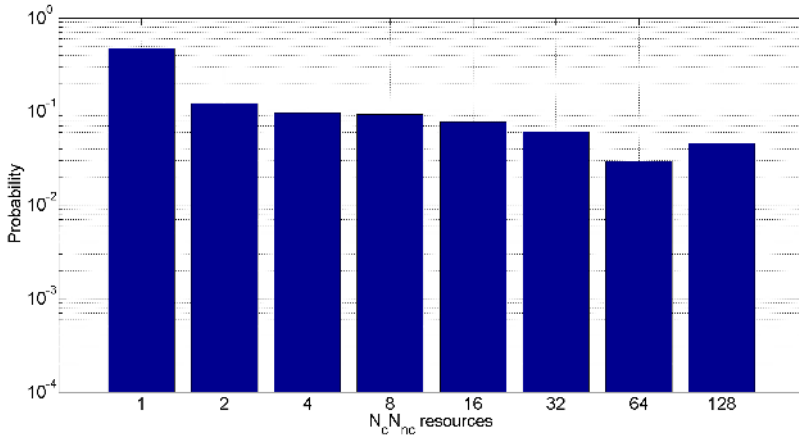
Figure 4.15: *Distribution of repetitions for users with the bad indoor case in cells with inter-site distance 5000 m*

Inter-site distance [m]	$R_{average}$ [repetition/succesful transmission]
500	1.00
1732	1.19
2500	1.91
5000	14.36

Table 4.2: *Random access preamble sequence length*

$$G = \frac{P_{\text{eNB}} \cdot g_{\max}}{\sum\limits_{i \in A} P_{\text{eNB}} \cdot g_i + N_{\text{dl}}}. \tag{4.4}$$

where P_{eNB} is the maximum power of the serving eNodeB. g_i is the path gain from a fixed location to eNodeB with index i, and A is the set indices of the path gains where the index of the maximum path gain, g_{max} is excluded. The term N_{dl} is the thermal noise in the downlink. The reason there are two different noise terms for uplink and downlink is because of hardware differences in the UE and eNodeB.

The reason for using geometry in the downlink and SNR in the uplink is because of the fundamental differences between the two cases. In the uplink, neighboring eNodeBs can coordinate the uplink transmission so that SNR limited users in one cell covered by an eNodeB uses the same frequency as users close to neighboring eNodeBs. The users close to neighboring eNodeBs can then transmit with lower power and avoid interfering the SNR limited users. In the downlink, the eNodeBs use full power. The eNodeBs could use coordination where they avoid transmitting on certain frequencies, but this results in decreased capacity. This can be seen in the Shannon–Hartley theorem (4.5).

$$C = B \log_2 (1 + \text{SNR}). \tag{4.5}$$

If the bandwidth is decreased, the increase of SNR needed to keep the same capacity is much higher for high SNR as the capacity increases logarithmically with the SNR. In most cases, it is instead more efficient to use full bandwidth with some interference as a result, leading to a slightly lower SNR in downlink. In total, it will in most cases still lead to higher capacity than in the case of avoiding certain frequencies in the downlink.

Figures 4.16 - 4.19 show the results of the geometry in downlink for the four inter-site distances used and Figure 4.20 shows all the inter-site distances plotted against each other in the bad indoor case. The output power is assumed to be 4.8 W over the bandwidth 1.08 MHz (6 RB) and the uplink noise figure, F_{dl}, is set to 9 dB.
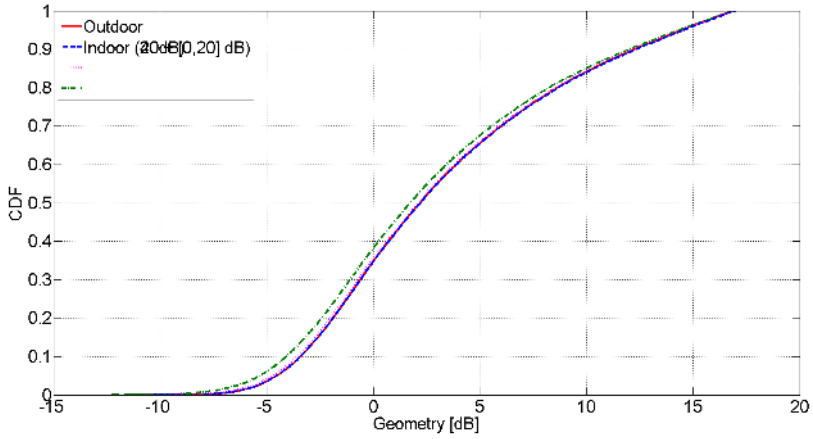
Figure 4.16: *CDF-plot of the geometry in downlink for inter-site distance 500 m.*
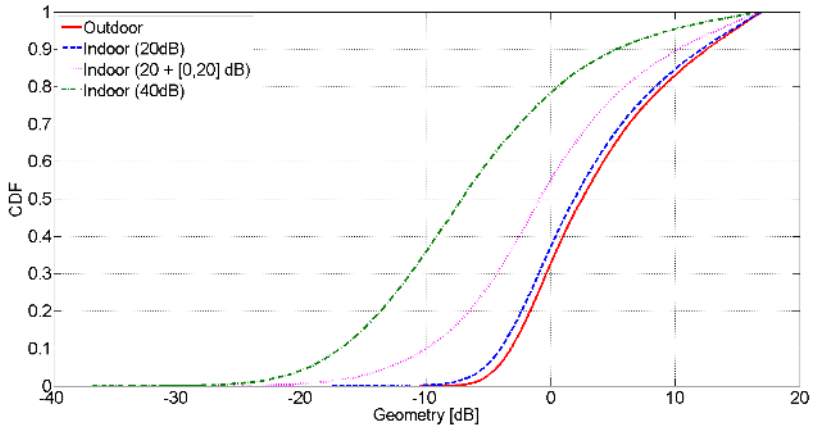

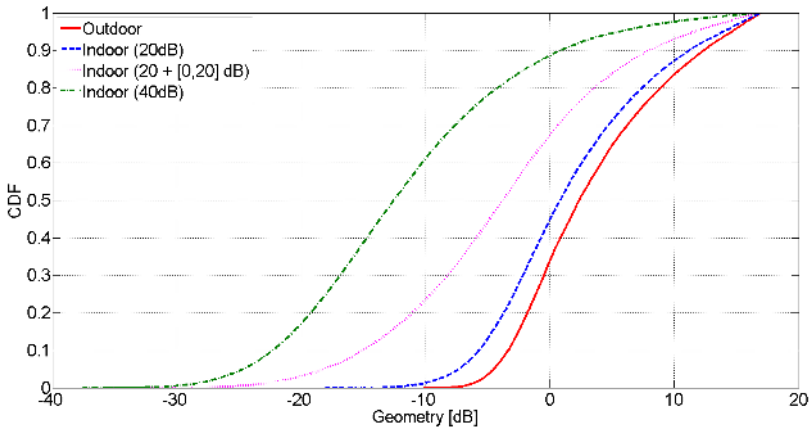**Figure 4.17:** *CDF-plot of the geometry in downlink for inter-site distance 1732 m.*

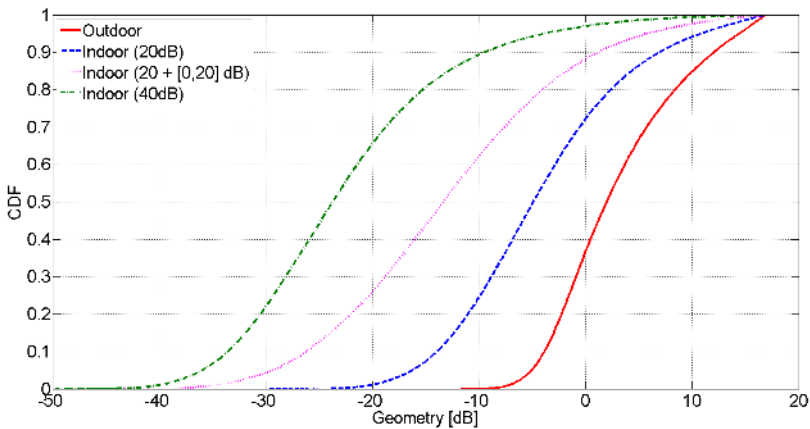**Figure 4.18:** *CDF-plot of the geometry in downlink for inter-site distance 2500 m.*

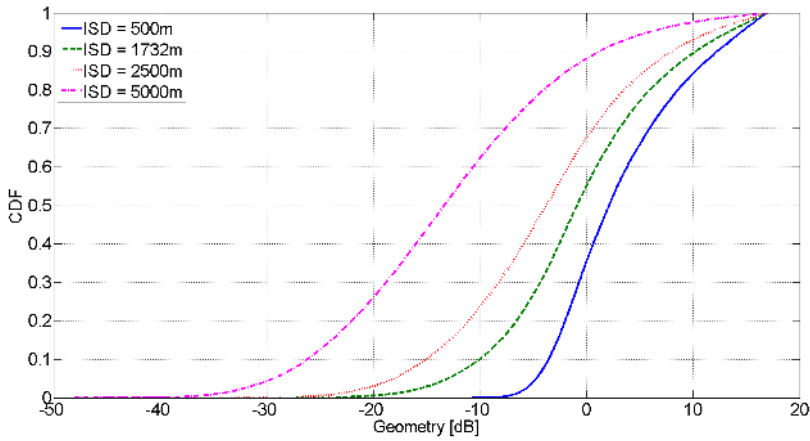**Figure 4.19:** *CDF-plot of the geometry in downlink for inter-site distance 5000 m.*

Figure 4.20: *CDF-plot of the geometry in downlink for different inter-site distances for the bad indoor case.*

The difference between the plots in the geometry case is much more significant than in the SNR case. The general pattern in the geometry plots is that the geometry distribution for the different users are more similar for shorter inter-site distances while they differ a lot for longer inter-site distances. The reason for this is the interference term in the denominator in Equation 4.4. For short inter-site distances, the signal power factor in the numerator is large, which means that also the interference term is large. The interference will thus dominate the denominator. This means that the users are mainly interference limited. In the case of longer inter-site distances, the interference factor is less significant compared to the interference in the noise limited case, making the users less interference limited and more noise limited.

As can be seen in Figure 4.20, the shapes for the different inter-site distance cases are quite different, with shorter inter-site distances resulting in a steeper curve. This is the result of the different effects of interference and noise for different inter-site distances.

The differences of the results in Figure 4.12 and 4.20 show that the uplink is much more limited than the downlink. This can be seen from the distribution of the uplink SNR being more concentrated at lower SNR than the downlink. The conclusion of this is that the uplink will need more resources compared to the downlink.

4.3   PUSCH Simulation

The simulations for evaluating the performance of the PUSCH are divided into two parts, where each part is based on different assumptions. The first part is

based on link simulations from [16] and the second part is simulated in the system simulator.

4.3.1 Estimated PUSCH Link Performance

The data from [16] is the result from a link simulator and shows the downlink data rate for certain SNR. Figure 4.21 shows the results from [16]. The results presented in this section are based on the same simulator with slightly different parameters according to Table 4.3 for low SNR and the results from [16] for high SNR. This is a somewhat rough assumptions but the results have showed that the differences are not that big. The assumed number of pilots is based on only one transmitter antenna.
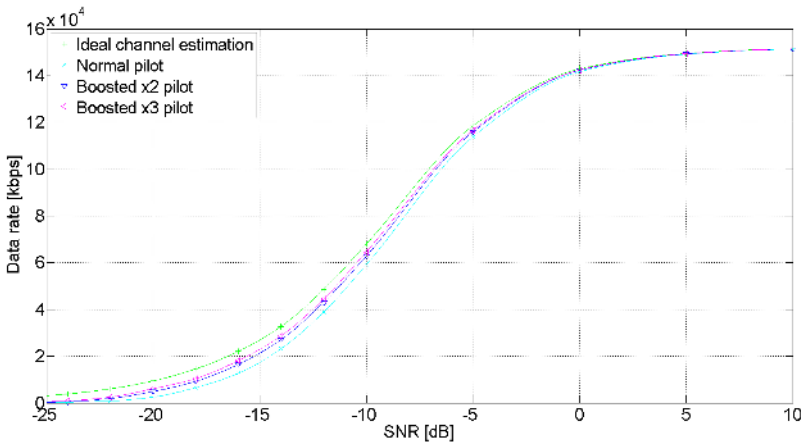
Figure 4.21: Downlink link simulation results from [16].

MCS 0 means that the modulation used is QPSK and that the transport block size is 152 bits over 6 PRB [5]. The definition of the EPA channel model can be found in [2]. In this subsection, the downlink results are used to estimate the uplink performance. The translation into corresponding uplink data rate is a rough estimation and is purely based on the performance on the PDSCH and the differences in overhead.

In the PDSCH, three OFDM-symbols are assumed to be the control region, which together with an additional 6 resource elements of pilots constitutes the overhead per RB pair. The overhead is thereby $dl_{oh} = \frac{3 \cdot 12 + 6}{12 \cdot 14}$. In the PUSCH, the overhead consists of two OFDM-symbols pilots which makes the overhead: $ul_{oh} = \frac{2 \cdot 12}{12 \cdot 14}$. The amount of data per RB pair in the PUSCH compared to the PDSCH is then $\frac{1 - ul_{oh}}{1 - dl_{oh}} \approx 1.14$.

As the PDSCH is modeled as 6 RB in frequency and the PUSCH, 1 RB, the uplink data rate is calculated as $\frac{1 - ul_{oh}}{1 - dl_{oh}}/6 \approx 0.19$ of the downlink data rate. The amount of pilot power in the uplink is three times greater than in the downlink which

Parameter	Value
Number of subframes	20000
System Bandwidth	1.4 MHz
Frame Structure	FDD
Carrier frequency	2.0 GHz
Antenna configuration	1Tx, 2Rx, low correlation for FDD
Channel model	EPA
Doppler spread	1 Hz
MCS	0
Number of allocated DL PRBs	6
HARQ	2 HARQ-processes with RTT=2TTI
Frequency error	20 Hz
Performance target	10 % BLER for the initial HARQ transmission
Channel estimation	Frequency domain FIR filtering and time domain IIR filtering with memory between subframes (or ideal)

Table 4.3: FDD PDSCH link simulation assumptions

means that the corresponding uplink speed should be compared with the downlink curve in the case of a factor 3 power boost of the pilot symbols. The resulting graphs are shown in Figure 4.22 and shows the performance for the case of ideal channel estimation in downlink, channel estimation with normal pilot power in downlink, channel estimation with an increased pilot power in downlink and normal channel estimation in the uplink. The channel model is further explained in [2, p. 63].

By mapping the data rate for a certain SNR to the SNR distributions from Section 4.1.4 with the frequency adjusted to one RB and with the bad indoor case, the coverage and average data rate for the users are gained. The average repetition, data rate, transmission time and coverage are presented in Table 4.4, where 1064 bits per user were sent. The repetition increase is the average amount of extra repetition needed for the enhanced coverage compared to today's LTE. Note that the effective delay will be larger if the bits are not sent in consecutive subframes.

ISD [m]	Repetition	Repetition increase [%]	Data rate [kbps]	LTE coverage [%]	Enhanced coverage [%]
500	1.0014	0.0	28.720	99.9588	100
1732	1.1854	14.9	24.260	75.1375	99.9918
2500	1.4256	36.4	20.173	55.3927	99.7828
5000	2.6322	147.9	10.926	19.7971	91.5466

Table 4.4: Results from the uplink transmission.

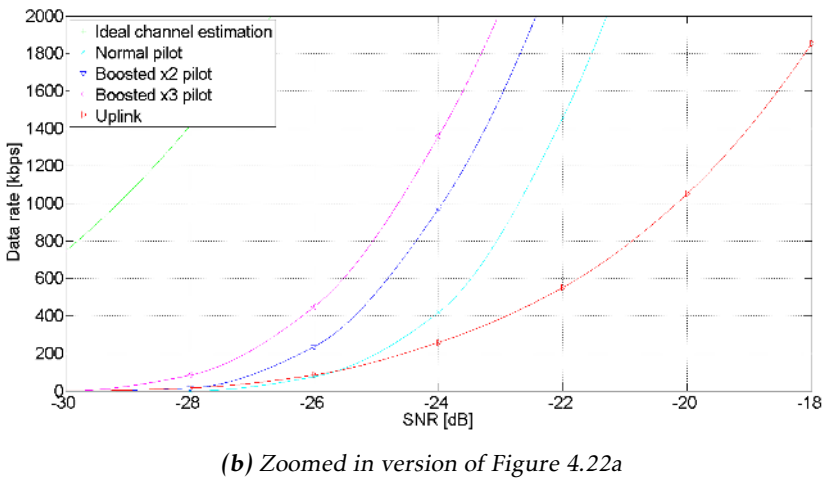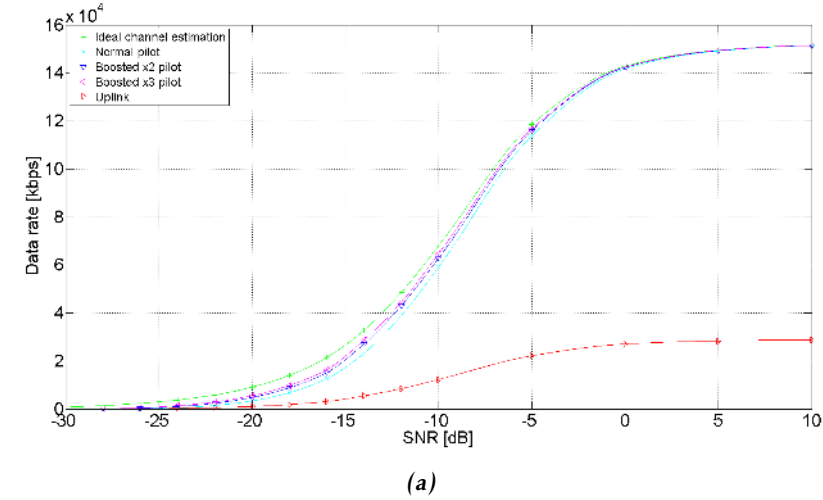*(a)*

(b) Zoomed in version of Figure 4.22a

Figure 4.22: *Simulated downlink and estimated uplink data rates for PDSCH and PUSCH.*

As can be seen in Table 4.4, the increase of coverage due to repetition is immense. The coverage for users with the bad indoor case in a cell with inter-site distance 2500 m has increased from 44.5% to 99.8%. It shows that the increased link budget makes a big difference in the pursuit of providing coverage for the users with bad channel conditions.

The repetition corresponds to the repetition needed compared to the users with best SNR. As the users with best SNR have a bit rate of 28.7717 kbps, the number of bits per RB pair becomes 28.7717. Since each uplink RB in the case of PUSCH

transmission contains two OFDM-symbols pilots, the code rate becomes

$$28.7717/(12 \cdot 12 \cdot 2) \approx 0.1.$$

With the following assumptions, the number of users supported can be calculated.

- Each user transmits 1064 bits (PHY) once per hour.
- 50 RB (10 MHz) is available for uplink.
- The full uplink bandwidth is used for transmission for the MTC-devices.
- The resources can be perfectly allocated to all the users.
- The users are assumed to already have a connection setup.

The results with and without imperfection assumptions are summarized in Figure 4.23.
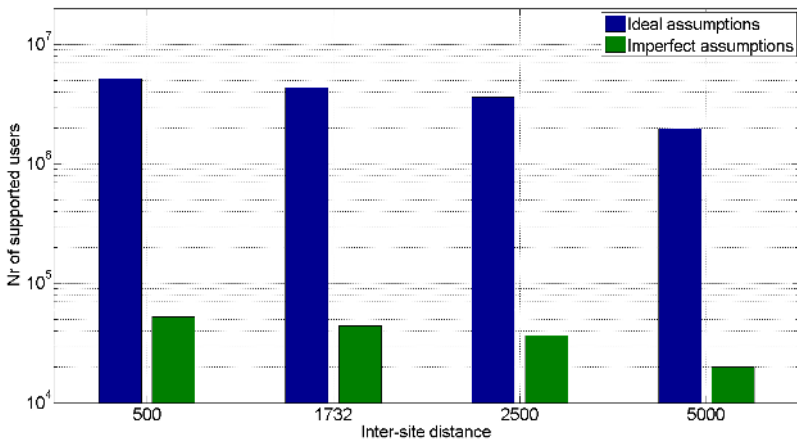
Figure 4.23: *Number of MTC-devices supported per cell with the bad indoor case.*

Note that the results without imperfection assumptions should be considered an upper bound for the number of users supported. There are some factors which will decrease the actual values. Some of them are:

- MTC-devices would typically not be assigned all resources.
- The scheduling of the resources would not be optimal.
- The intensity of reports from the MTC-devices could be denser.
- Connection setup and control signaling may require a significant portion of the uplink resources.

As most of the traffic today in LTE is human centric with high requirements on data rate and delay, a large portion of the resources would typically be assigned to high-end users rather than the low-end users. The scheduling of the resources to different users would typically not be perfect. This includes the fact that the intensity of the devices would not be distributed uniformly in time. In the case where many devices transmit on the RACH simultaneously, collisions might occur, leading to non-optimal handling of the resources. As the transmission from users requiring very high number of repetitions occur relatively seldom, some of the assigned RACH resources might not be used.

Transmitting approximately 1000 bits per hour could be considered too sparse, which would further decrease the number of users. The resources used in the connection setup will require additional resources, but as shown in Table 4.2, the amount of resources needed for the first step of the random access procedure is small compared to the transmission of the 1000 bits. The same applies for the other steps in the random access procedure. Control signaling would be needed, and with repetition as well but the resources needed are also small compared to the 1000 bits.

Even though there are some factors leading to a decrease of the number of users supported, it still results in a high number. The imperfection assumptions used to generate some of the data in Figure 4.23 are defined as:

- Using only one tenth of the frequency in the uplink.

- Having an 50% scheduling imperfection.

- Having four times more dense transmissions.

- Having 20% of the resources used for connection setup and control signaling.

As can be seen, even with rough imperfection assumptions, the number of users supported is still relatively high which shows that supporting MTC-devices is not user limited, but rather coverage limited. Even with imperfect assumptions, the number of supported users in a cell with inter-site distance 5000 m are 19666.

As seen in Table 4.4, the coverage increase is immense, but for longer inter-site distances, the coverage is still a problem. For inter-site distances up to 2500 m, the coverage is almost complete. The coverage limitation at longer inter-site distances could however be acceptable as the coverage increase would imply coverage for a large number of users leading to extra resources at only a few locations.

4.3.2   System Simulated PUSCH

In the second part of the uplink data rate calculation, the system simulator from Section 4.1.4 has been used. The inter-site distances of interest are the same as before, 500 m, 1732 m, 2500 m and 5000 m. The generated users had path losses according to the bad indoor case. Each created user is assumed to be synchronized and have a connection to the network and the channel of interest is the PUSCH. Control signaling and HARQ feedback on the PDCCH and PHICH is

assumed to arrive without failures. During the simulation, only one site and one user was simulated at a time.

The IP packets sent over the PUSCH were 1000 bits which results in transport block sizes of 1040 bits because of PDCP, RLC and MAC headers. The transport blocks were sent over 1 RB in frequency, which is not supported by today's LTE. However, as the relative cost of MAC headers is more expensive for small transport blocks, having one larger transport block instead of several smaller is desirable. A full description of the important parameters are presented in Table 4.5.

Parameter	Value
Frame Structure	FDD
Carrier frequency	2.0 GHz
Antenna configuration	1Tx, 2Rx
Channel model	EPA
Number of allocated UL PRBs	1
Transport block size	1040 bits
Pilot symbols per RB pair	24
PHY CRC length	24 bits

Table 4.5: *FDD PUSH system simulation assumptions*

A repetition factor 1 is defined as transmitting the transport block of 1040 bits with CRC five times with 1 RB in frequency. Two OFDM-symbols per RB pair are used as uplink demodulation reference signals, and the modulation used is QPSK. This gives a code rate of $\frac{1064}{12 \cdot (14-2) \cdot 5 \cdot 2} \approx 0.7389$, which could be considered an aggressive code rate as a first attempt for coverage limited users. Repetition factors 2, 4, 8, 16, 32, 64, 128, 256, 512 and 1024 are the repetitions relative repetition factor 1 of the transport block with the soft information being accumulated at the eNodeB, which in the simulation defines when the users are allowed to decode. When transmitting the data, the RB pairs are separated 8 ms for diversity.

According to [9, Table 5.2.1.2-2], today's LTE can support data rates on the PUSCH down to 20 kbps at an SNR of -4.3 dB. The desired 20 dB increase is relative this point of operation. The bandwidth in [9] corresponds to two RB in frequency which means that if the energy would be focused over 1 RB, 3 dB are achieved.

20 kbps on two RB in frequency translates into 10 bits per RB pair which with QPSK results in a code rate of $\frac{10}{12 \cdot 12 \cdot 2} = 0.0347$. As 3 dB are gained from concentrating the energy in frequency, an increase of 17 dB from repetition results in a code rate of $\frac{10}{12 \cdot 12 \cdot 2 \cdot 50} \approx 6.94 \cdot 10^{-4}$. The repetition factor 1024 results in a code rate of $7.22 \cdot 10^{-4}$ which is roughly the desired code rate.

As repetition factor 1 implies a data rate of $\frac{1064}{0.005} = 212.8$ kbps, the highest repetition factor 1024 corresponds to a data rate of $212800/1024 \approx 208$ bps. The highest repetition factor supported by today´s LTE corresponds to 10.6, but will because of the discrete repetition factor values be set to 8. Today's LTE coverage

will thus be measured as the amount of users requiring a repetition factor of 8 or less.

Figure 4.24-4.27 show the results from the simulation. In these results, the fast fading effects has been taken into account, unlike Section 4.1.4.
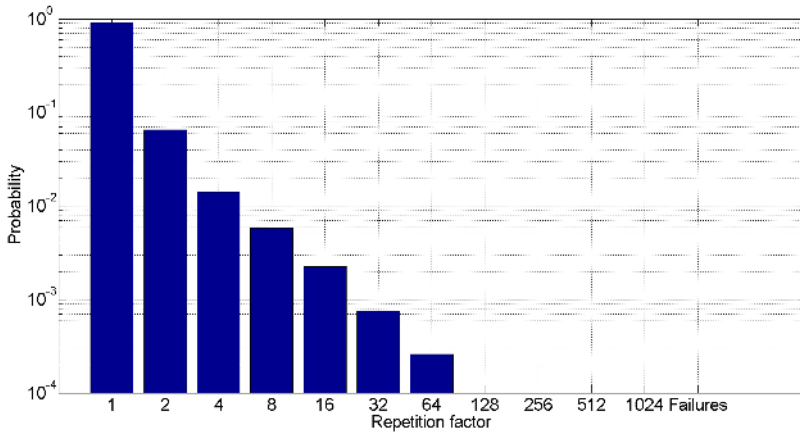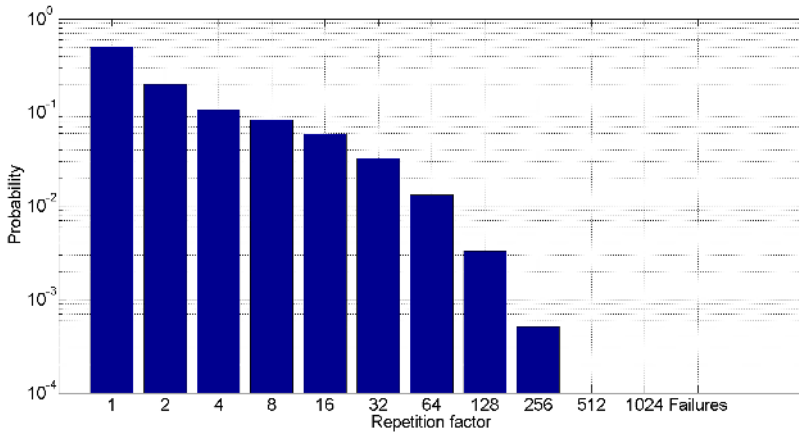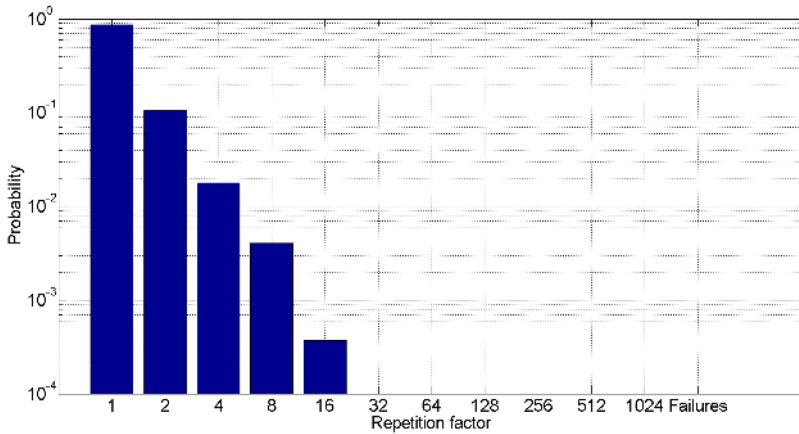

(a) Bad indoor case.
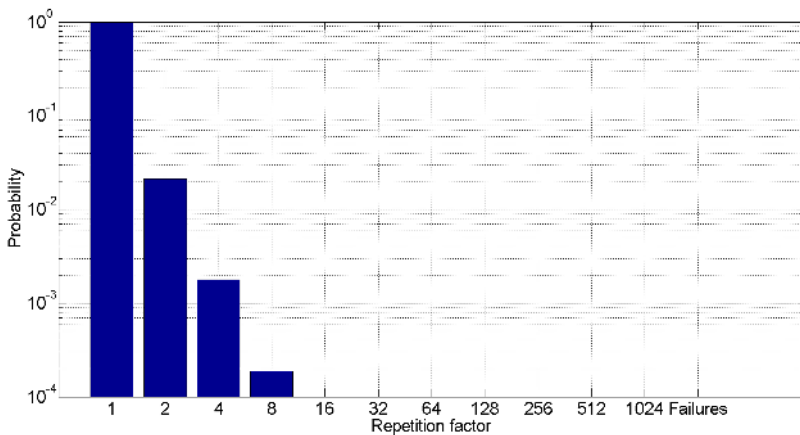
(b) Indoor case.

Figure 4.24: *Repetition distribution for inter-site distance 500 m.*

As can be seen in the figures, the differences between the results from different inter-site distances as well as from users with and without additional path loss are significant. The statistics of Figure 4.24-4.27 is presented in Table 4.6 for the bad indoor case. The repetition increase is the average amount of extra repetition needed for the enhanced coverage compared to users needing only repetition factor 1–8.

(a) Bad indoor case.

(b) Indoor case.

Figure 4.25: *Repetition distribution for inter-site distance 1732 m.*

ISD [m]	Repetition	Repetition increase [%]	Data rate [kbps]	LTE coverage [%]	Enhanced coverage [%]
500	1.2428	8.2	171.23	99.6618	100
1732	5.4046	141.1	39.374	89.1540	100
2500	44.5591	1432.7	4.7757	62.9272	99.2069
5000	158.6891	4160.4	1.3410	28.6359	90.2120

Table 4.6: *Results from the uplink transmission.*

The coverage increase for coverage limited MTC-devices by repetition is immense, especially for longer inter-site distances.

Figure 4.28 shows the results of the number of users supported for the cases
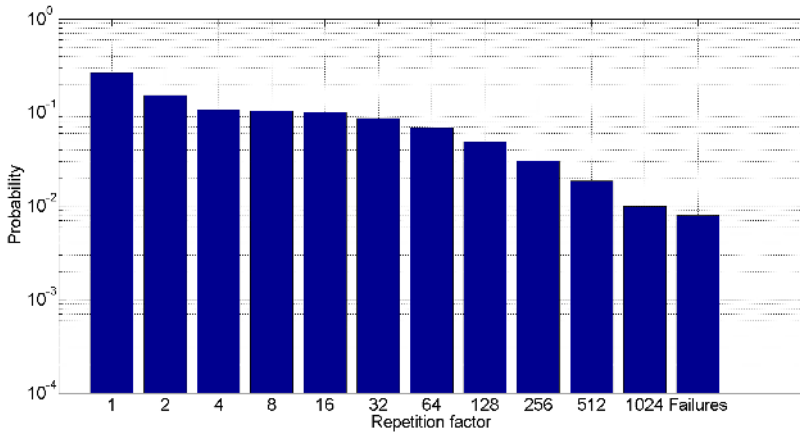
(a) *Bad indoor case.*
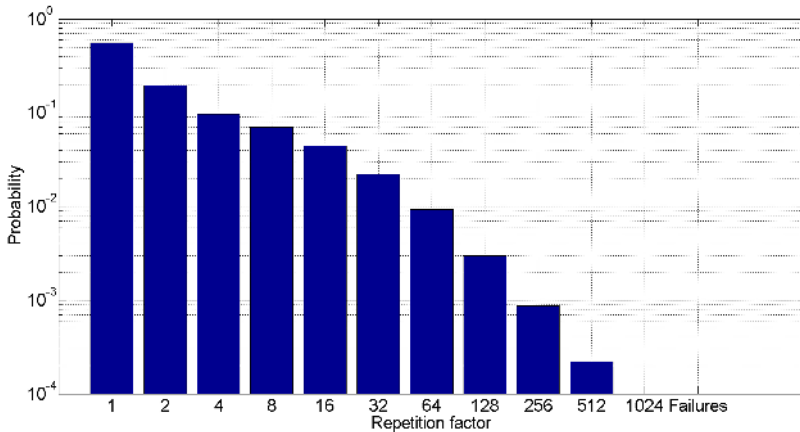
(b) *Indoor case.*

Figure 4.26: *Repetition distribution for inter-site distance 2500 m.*

indoor and bad indoor, with and without the imperfection assumptions from the previous section.

Also the system simulated part of the PUSCH simulation shows that the number of supported users are high, even with rough imperfection assumptions. The number of supported users in the bad indoor case with imperfection assumptions and inter-site distance 5000 m is 2413. In the cases where base stations are located with such distances, the users are usually sparsely located meaning that 2413 is a high number. For shorter inter-site distances, the number of users is much higher as seen in Figure 4.28.
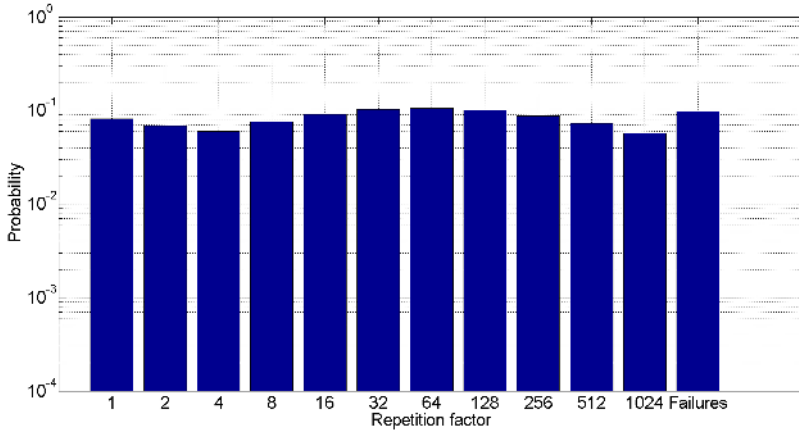
(a) Bad indoor case.
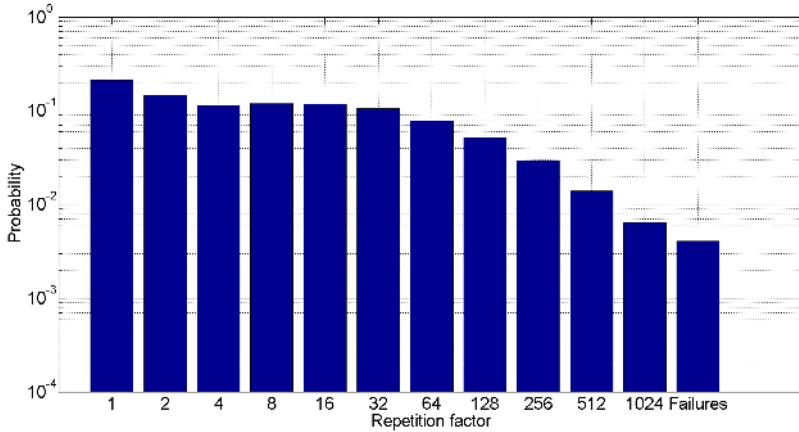
(b) Indoor case.

Figure 4.27: *Repetition distribution for inter-site distance 5000 m.*

Just as in the previous subsection, the coverage increase is significant. For inter-site distances up to 2500 m, the coverage for users with the bad indoor case is almost complete and even with inter-site distance 5000 m, the coverage is 90.2%. Once again, it shows that an increase of 20 dB by means of repetition does provide a high coverage at a low cost, implying that the limitation is on the coverage rather than the number of users supported.
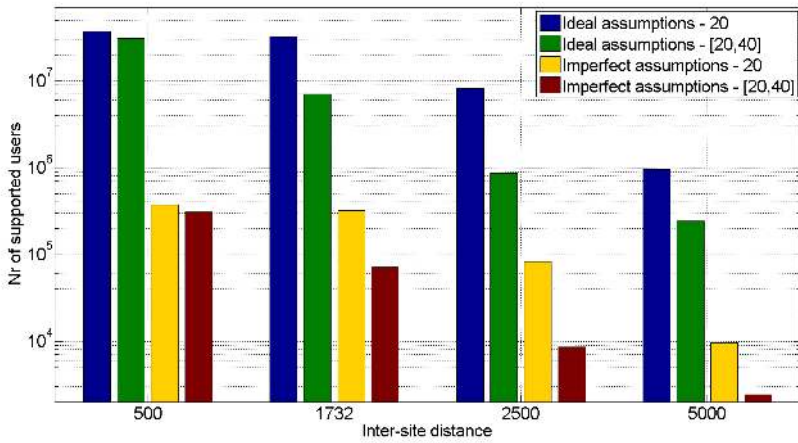
***Figure 4.28:** Number of users supported.*

5

Discussion

5.1 Conclusion

As shown in Chapter 4, it is possible for a significant coverage increase for coverage limited users at a low cost. For inter-site distances up to 2500 m, an SNR increase of 20 dB leads to an almost complete coverage for coverage limited MTC-devices as well as fulfilling their needs of data rate and delay, as compared to today's LTE.

Section 4.3 showed that with an inter-site distance of 2500 m, the coverage can be improved from around 55.4-62.9% to 99.2-99.7% with the possibility to theoretically support more than 10^4 users in terms of resources even with imperfect assumptions. This coverage improvement was possible with an increase of 20 dB, which also fulfilled the requirements of the MTC-devices. This coverage improvement is possible because of the small infrequent transmissions by the MTC-devices with relaxed delay constraints.

Section 4.1 showed that also the preamble transmission during the random access procedure can be done at low SNR with repetition.

It was also shown that the limitation lies in the coverage rather than the number of users supported, as the type of users considered in this thesis have such low requirements. This means that the coverage limited MTC-devices can be offered a connection at a very low cost. The coverage increase by means of repetition also allow for non-hardware upgrades which is an important factor when considering coverage enhancement options.

5.2   Future Work

The main focus of this thesis has been on the uplink as it is the most limited part of the communication for the devices of interest in this thesis. It would however be interesting to consider all the signaling steps in both uplink and downlink from synchronisation and transmission on the shared channels to transmission on the control channels.

It would also be interesting to analyze the effects of interference in the uplink to see how this affects the energy accumulation.

As the additional repetition will lead to more signal processing, it is of interest to consider the energy consumption.

Appendix

A

Simulation Details

A.1   Preamble Detection Link Simulation Setup Details

The SNR in the preamble link simulation is defined as the ratio between the power of one preamble and the corresponding noise with the bandwidth,

$$N_{ZC} \cdot \Delta f_{RA} \approx 1.05 \text{ MHz}.$$

The SNR can equivalently be expressed as the ratio between the power of one preamble subcarrier and the corresponding noise. The number of carriers in the preamble, N_{ZC}, is 839, which means that the gain compared to one carrier is $10 \cdot \log_{10}(839)$dB.

The thermal noise power is defined as $N = kFT_0B$, where $k = 1.38 \cdot 10^{-23}$J/K is the Boltzmann constant, $T_0 = 290$K is the reference temperature, B is the bandwidth and F is the noise figure which depends on the hardware. In downlink, the noise figure, F_{dl} is set to 9dB [9] and in the uplink, F_{ul} is set to 5dB [9]. The reason for that is that the hardware is typically better in eNodeBs compared to UEs. The variance of the noise is the same as the power; $\sigma_n^2 = kF_{ul}T_0B$.

At the receiver, the signal passes a normalized matched filter and the output of the kth preamble with coherent accumulation N_c can be written as

$$r_k^{(N_c)} = N_c \cdot L \cdot h_k \sqrt{P} \cdot S + n_k, \tag{A.1}$$

where L is the path loss, h_k is the factor from the Rayleigh fading, P is the power of the terminal and $S \in \{0, 1\}$ corresponds to whether a signal was sent or not. r_k is the received component after the transmission of a single preamble. n_k is the noise component and is a stochastic variable with variance $\sigma^2_{n_{\text{tot}}}$ and mean 0. The way S is modeled implies that two different preambles are assumed to have zero correlation, which is how the correlation effect of the Zadoff-Chu sequences is modeled. In reality, different preambles sent on the same resources will have a non-zero impact on one another.

Equivalent ways of expressing the SNR is shown below

$$\text{SNR} = \frac{L^2 \cdot \sigma_h^2 \cdot P}{\sigma^2_{n_{\text{tot}}}} = \frac{L^2 \cdot P}{\sigma^2_{n_{\text{tot}}}} = \frac{\sum_{p=1}^{N_{ZC}} s^2_{\text{single}}}{\sum_{p=1}^{N_{ZC}} \sigma^2_{n_{\text{single}}}} = \frac{s^2_{\text{single}}}{\sigma^2_{n_{\text{single}}}}. \tag{A.2}$$

$\sigma^2_{n_{\text{tot}}}$ is the variance of the noise over the total bandwidth, $\sigma^2_{n_{\text{single}}}$ is the variance of the noise over 1250 Hz and s^2_{single} is the signal power of one subcarrier.

Since h is assumed to have variance 1, the factor σ_h^2 can be omitted. The path loss can then be written as

$$L = \sqrt{\frac{\text{SNR} \cdot \sigma_n^2}{P}}, \tag{A.3}$$

which inserted in equation A.1 becomes

$$r_k^{(N_c)} = N_c \cdot \sigma_n \cdot \sqrt{\text{SNR}} \cdot h_k \cdot S + n_k. \tag{A.4}$$

As the noise for one subcarrier is: $\sigma^2_{n_{\text{single}}} = k \cdot F \cdot T_0 \cdot 1250$, the expression for the total noise becomes: $\sigma^2_{n_{\text{tot}}} = \sum_{i=1}^{N_{ZC}} \sigma^2_{n_{\text{single}}} = N_{ZC} \cdot \sigma^2_{n_{\text{single}}}$.

The amplitude of the total signal component including coherent accumulation and total variance is then

$$s_{tot} = N_c \cdot N_{ZC} \cdot s_{\text{single}} = N_c \cdot N_{ZC} \cdot \sigma_{n_{\text{single}}} \cdot \sqrt{\text{SNR}}, \text{and} \tag{A.5}$$

$$\sigma_n^2 = N_c \cdot \sigma^2_{n_{\text{tot}}} = N_c \cdot N_{ZC} \cdot \sigma^2_{n_{\text{single}}}. \tag{A.6}$$

The total effective SNR becomes

$$\text{SNR}_{\text{effective}} = \frac{s_{tot}^2}{\sigma_n^2} = N_\text{c} \cdot N_{\text{ZC}} \cdot \text{SNR}. \tag{A.7}$$

Since the phase difference is not known in the case of non-coherent accumulation, the absolute values of the signal components with noise are added together. This means that the total received component becomes

$$r = \sum_{k=1}^{N_{\text{nc}}} |r_k^{(N_\text{c})}|. \tag{A.8}$$

The channel quality for $r_k^{(N_\text{c})}$ and $r_j^{(N_\text{c})}$ are for $k \neq j$ assumed to be independent, which gives rise for time diversity, which partly will counter the effect of the Rayleigh fading. This is a somewhat rough assumption since the correlation between the channel conditions on different time instances will depend on the difference in time.

The receiver is assumed to have two uncorrelated antennas which makes the effective N_{nc} twice as big.

A.2   Link Simulation

```
BOLTZMANN_CONSTANT = 1.38*10^{-23}
NOISETEMPERATURE = 290
NOISEFIGURE = 10^(5/10)
NR_RACHPR = 839
BW_RACH_PREAMBLE = 1250
BW_TOT = BW_RACH_PREAMBLE * NR_RACHPR
% Power of the noise.
ULNOISEFLOOR_SINGLE = BOLTZMANN_CONSTANT * NOISETEMPERATURE *
    NOISEFIGURE * BW_RACH_PREAMBLE
ULNOISEFLOOR_TOT = BOLTZMANN_CONSTANT * NOISETEMPERATURE *
    NOISEFIGURE * BW_TOT
% Standard deviation for the noise over 1250Hz.
SIGMA_N_SINGLE = sqrt(ULNOISEFLOOR_SINGLE)
% The variance of a sum of stochastic variables with covariance
    0 for each pair is the sum of the variances. The standard
    deviation used is for the whole bandwidth.
SIGMA_N_TOT = sqrt(Nc)*sqrt(ULNOISEFLOOR_TOT)
% Signal amplitude with Nc coherent accumulations.
S = Nc * NR_RACHPR * SIGMA_N_SINGLE * sqrt(SNR)
for iteration = 1 to number of iterations
    h = 1/sqrt(2)*complex(randn(2*Nnc,1),randn(2*Nnc,1))
    n = sigma_n_tot/sqrt(2)*complex(randn(2*Nnc,1),randn(2*Nnc,1))
    received_signal = h*S + n
    % Add the amplitudes of the Nnc versions
```

```
Z(i) = sum(abs(received_signal))
$Z_0$(i) = sum(abs(n))
```

The pseudo code above illustrates how the link simulation in Section 4.1 was performed.

By making many such simulations, the distribution of the signals was gained. To get a more intuitive view of the performance for different values of N_{nc}, histograms of the results is presented in Figure A.1. The x-axis shows A.8 for the cases when the signal was sent and not sent, scaled with the number of repetitions. The probability for a miss/false detection is then calculated by placing the threshold so that the probabilities are equal, and considering the area on each side of the threshold.
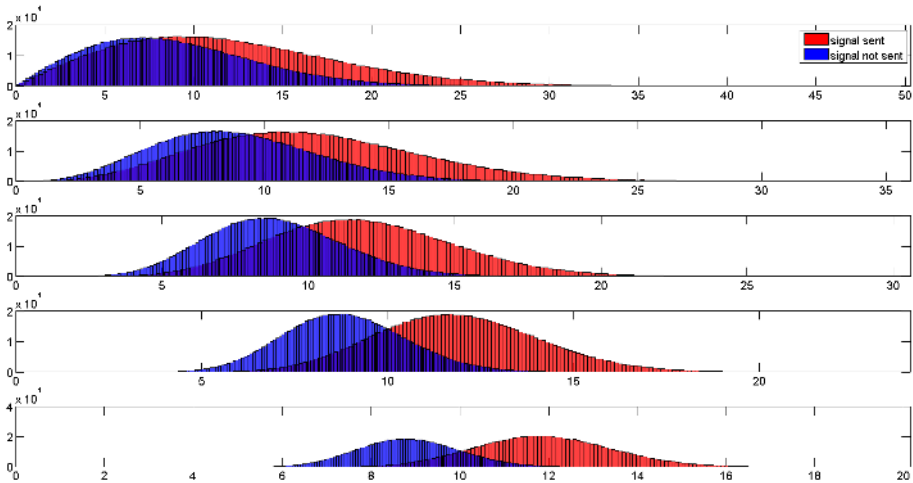
Figure A.1: *Histograms of the link simulations for $N_c = 1$ and $N_{nc} = \{1, 2, 4, 8, 16\}$*

A.3   System Simulation

When calculating R_k for the percentage of the users of interest, each user in that set is mapped to an error probability and values of N_c and N_{nc} according to figure A.2. With those values, the average repetitions for a successful transmission, R_k, is calculated according to equation 4.3. The total average R is then calculated by averaging R_k over the number of users in the simulation.
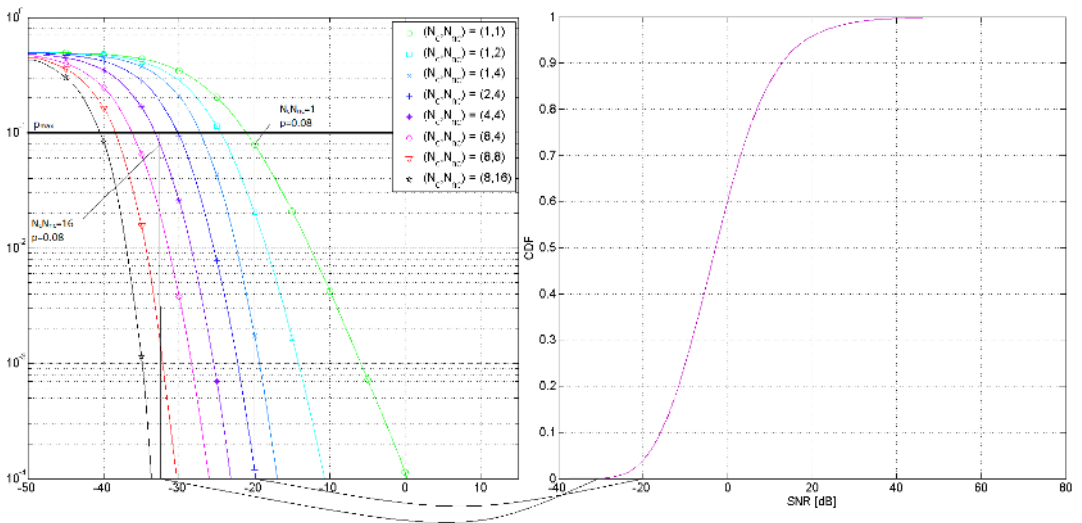
Figure A.2: *Illustration of mapping from SNR to repetition and error probability*

Bibliography

[1] 3GPP. *Requirements for Evolved UTRA (E-UTRA) and Evolved UTRAN (E-UTRAN)*. Number TR25.913 in TR. January 2009. URL `http://www.3gpp.org/ftp/Specs/html-info/25913.htm`. Rel-8 v8.0.0. Cited on page 3.

[2] 3GPP. *Evolved Universal Terrestrial Radio Access (E-UTRA); Base Station (BS) radio transmission and reception*. Number TS36.104 in TS. September 2009. URL `http://www.3gpp.org/ftp/Specs/html-info/36104.htm`. Rel-9 v9.1.0. Cited on pages 42 and 43.

[3] 3GPP. *Evolved Universal Terrestrial Radio Access (E-UTRA); Physical channels and modulation*. Number TS36.211 in TS. September 2009. URL `http://www.3gpp.org/ftp/Specs/html-info/36211.htm`. Rel-8 v8.8.0. Cited on pages 9, 10, 14, 17, and 18.

[4] 3GPP. *Evolved Universal Terrestrial Radio Access (E-UTRA); Multiplexing and channel coding*. Number TS36.212 in TS. June 2009. URL `http://www.3gpp.org/ftp/Specs/html-info/36212.htm`. Rel-8 v8.7.0. Cited on page 13.

[5] 3GPP. *Evolved Universal Terrestrial Radio Access (E-UTRA); Physical layer procedures*. Number TS36.213 in TS. September 2009. URL `http://www.3gpp.org/ftp/Specs/html-info/36213.htm`. Rel-8 v8.8.0. Cited on page 42.

[6] 3GPP. *Evolved Universal Terrestrial Radio Access (E-UTRA) and Evolved Universal Terrestrial Radio Access Network (E-UTRAN); Overall description; Stage 2*. Number TS36.300 in TS. September 2009. URL `http://www.3gpp.org/ftp/Specs/html-info/36300.htm`. Rel-9 v9.1.0. Cited on pages 5, 6, and 7.

[7] 3GPP. *Requirements for further advancements for Evolved Universal Terrestrial Radio Access (E-UTRA) (LTE-Advanced)*. Number TR36.913 in TR. March 2009. URL `http://www.3gpp.org/ftp/Specs/html-info/36913.htm`. Rel-8 v8.0.1. Cited on page 3.

[8] 3GPP. Evolved Universal Terrestrial Radio Access (E-UTRA); Radio Resource Control (RRC);. (TS36.311), February 2010. URL http://www.3gpp.org/ftp/Specs/html-info/36331.htm. Rel-9 v9.1.0. Cited on page 15.

[9] 3GPP. Technical Specification Group Radio Access Network; Study on provision of low-cost MTC UEs based on LTE;. (TR36.888), June 2012. URL http://www.3gpp.org/ftp/Specs/html-info/36888.htm. Rel-11 v2.0.0. Cited on pages 32, 47, and 57.

[10] 3GPP. Evolved Universal Terrestrial Radio Access (E-UTRA); TDD Home eNode B (HeNB) Radio Frequency (RF) requirements analysis. (TR36.922), October 2012. URL www.3gpp.org/ftp/Specs/html-info/36922.htm. Rel-11 v11.0.0. Cited on page 25.

[11] Lars Ahlin, Jens Zander, and Ben Slimane. *Principles of Wireless Communications*. Studentlitteratur, 2008. Cited on page 31.

[12] CATT. Coverage improvement analysis for low-cost MTC UEs. (R1-130053), 2013. URL http://www.3gpp.org/ftp/tsg_ran/wg1_rl1/TSGR1_72/Docs/. Cited on pages 2 and 21.

[13] D.C. Chu. Polyphase codes with good periodic correlation properties. *IEEE T. Inform. Theory*, 18(4):531–532, 1972. Cited on pages 14 and 17.

[14] Erik Dahlman, Stefan Parkvall, and Johan Sköld. *4G LTE / LTE-Advances for Mobile Broadband*. Elseiver Ltd., 2011. Cited on page 3.

[15] Ericsson. More than 50 billion connected devices. 2011. URL http://www.ericsson.com/res/docs/whitepapers/wp-50-billions.pdf. Cited on page 1.

[16] Ericsson. Data Transmission For MTC Coverage Enhancements. (R1-130765), 2013. URL http://www.3gpp.org/ftp/tsg_ran/wg1_rl1/TSGR1_72/Docs/. Cited on page 42.

[17] Eriksson Erik. Channel quality information reporting and channel quality dependent scheduling in lte. Master's thesis, Linköping University. Cited on page 12.

[18] ITU-R. Requirements related to technical performance for IMT-Advanced radio interfaces. (M.2134), 2008. URL http://www.itu.int/dms_pub/itu-r/opb/rep/R-REP-M.2134-2008-PDF-E.pdf. Cited on page 3.

[19] F.J. MacWilliams and N.J.A. Sloane. Pseudo-random sequences and arrays. *IEEE T. Inform. Theory*, 64(12):1715–1729, 1976. Cited on page 14.

[20] Upamanyu Madhow. *Fundamentals of Digital Communication*. Cambridge University Press, 2008. Cited on pages 26 and 27.

[21] Vodafone. Study on Provision of low-cost MTC UEs based on LTE. (RP-

121441), 2012. URL `http://www.3gpp.org/ftp/tsg_ran/TSG_RAN.` `./TSGR_57/Info_for_workplan/revised_SID/`. Cited on page 2.